X-ray, Phase Space Density, and Velocity Dispersion Constraints on the Properties of the Dark Matter Particle:

Casey R. Watson
Millikin University
July 23, 2015

Many Thanks to
My Collaborators:
Peter Biermann (MPI, Univ. of Bonn, Univ of AL), Zhiyuan Li (CfA/UCLA/Nanjing University) & Joe Cheeney, Chris Pelikan, Nick Polley, Leon Yu (Millikin)
and
Norma Sanchez and Hector de Vega for inviting me.

OUTLINE

- **Phenomenology of Sterile Neutrinos**
- **Most Restrictive X-ray Constraints on Sterile Neutrinos:**
  - **The Advantages of Andromeda**
  - **Constraints from *XMM* Observations of Andromeda**
  - **Constraints from *Chandra* Observations of Andromeda**
- **The Bulbul et al. (2014) Anomaly in Context**
  - **vs. X-ray Constraints**
  - **vs. Galaxy Constraints**
- **Phase Space Density Constraints via MW dSphs**
  - **Implications for DM Particle mass**
- **Strong correlations between the half-light radii and dark matter halo parameters of MW dSphs**

The Fertile Phenomenology of Sterile Neutrinos

- **Non-zero active neutrino masses [1,2]**
- **Baryon & Lepton Asymmetries [15-20]**
- **Big Bang Nucleosynthesis [19]**
- **Evolution of the matter power spectrum [21,22]**
- **Reionization [23-31]**
- **Active Neutrino Oscillations [32-33]**
- **Pulsar Kicks [34-39]**
- **Supernovae [40-42]**
- **Excellent Dark Matter Particle Candidate [3-14, 43-57]**
- ***Most Importantly: Readily Testable***
  - ***Can decay into detectable X-ray photons***

Detecting Sterile Neutrino Radiative Decays:

$$\text{“}\nu_s\text{”} \rightarrow \text{“}\nu_\alpha\text{”} + \gamma$$

$$E_\gamma = \frac{m_s}{2} \sim 1 \text{ keV}$$

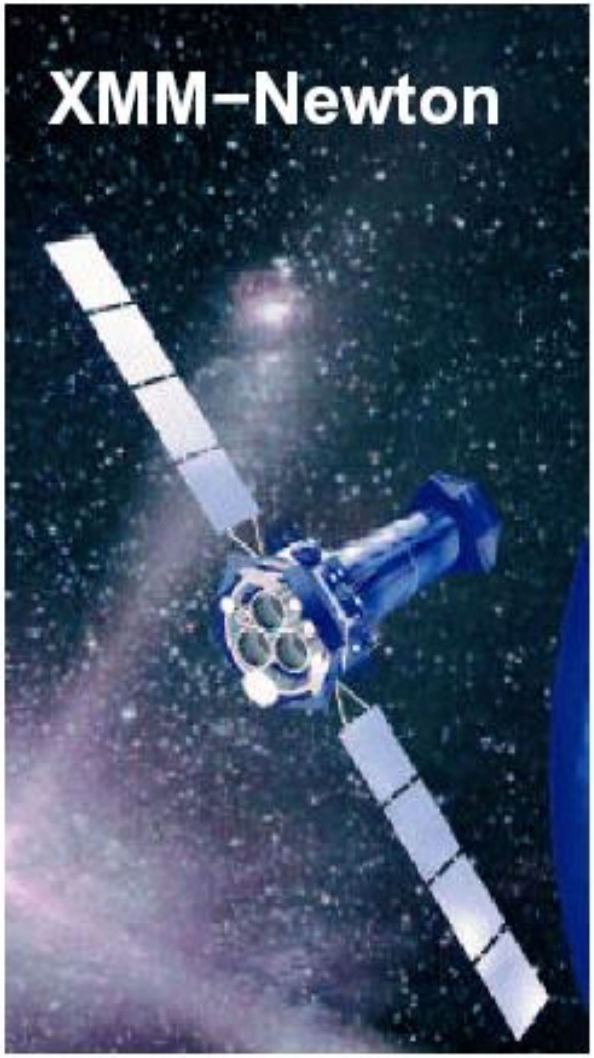

If

1 keV < m_s < 20 keV, *Chandra* & XMM can detect the X-ray photons associated with sterile neutrino radiative decays.

To maximize the sterile neutrino decay signal:

$$\phi_{x,s}(\sin^2 2\theta) \simeq 1.0 \times 10^{-17} \mathrm{erg\ cm^{-2} s^{-1}} \left(\frac{D}{\mathrm{Mpc}}\right)^{-2} \times \left(\frac{M_{DM}^{FOV}}{10^{11} M_\odot}\right) \left(\frac{\sin^2 2\theta}{10^{-10}}\right) \left(\frac{m_s}{\mathrm{keV}}\right)^{5}$$

the ideal object to study is:

- **nearby: small Distance D,**
- **massive: large M_{DM} (in FOV),**
- **quiescent: low astrophysical background.**

Astrophysical X-ray Sources:

Stellar Sources:

HMXB: Fueled by stellar wind; widely-separated

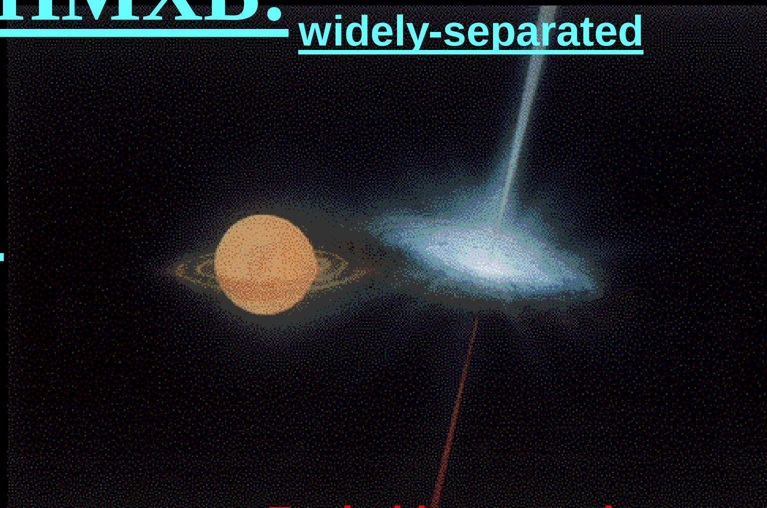

LMXB: Roche Lobe accretion; Contact Binary systems

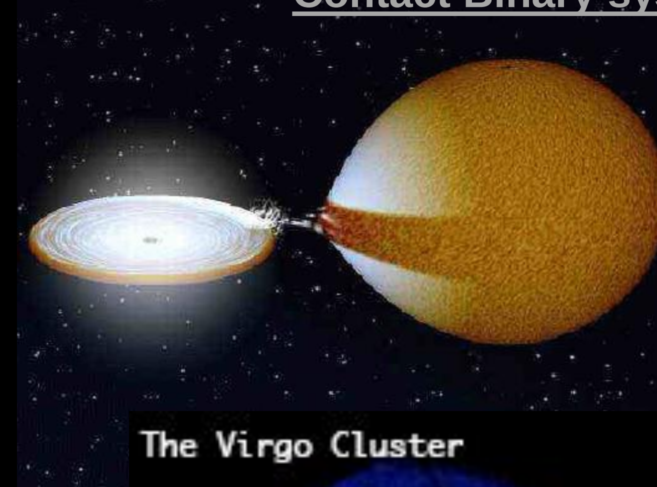

Nuclear & Diffuse Sources:

AGN: Fueled by accretion onto Supermassive BHs

Hot Gas:

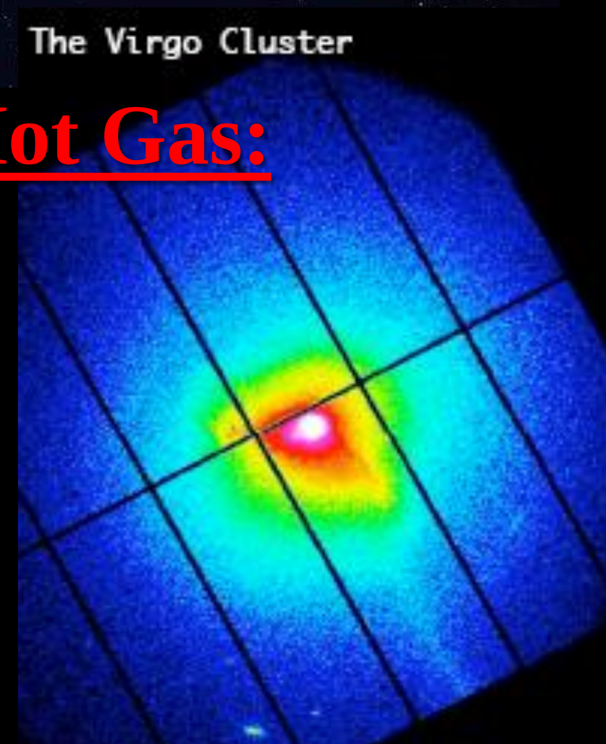

Advantages of Andromeda (M31)

(Watson, Li, Polley 2012, Watson, Beacom, Yuksel, Walker 2006 [66])

Nearby: D = 0.78 ± 0.02 Mpc [102, 103]

LOW astrophysical background (little hot gas & bright point sources can be excised)

Well-measured Dark Matter Distribution based on analyses of extensive Rotation Curve Data

(Klypin, Zhao, Somerville 2002 [104], Seigar, Barth, & Bullock 2007 [105])

Prospective Sterile Neutrino Signals

Comparable to Massive Clusters without the background

Exceed Ultra Nearby Dwarf Galaxies with better S/N

$$\frac{\Phi_{\mathrm{M31}}}{\Phi_{\mathrm{Clus}}} = \left(\frac{M_{M31}^{FOV}}{M_{\mathrm{Clus}}^{FOV}}\right)\left(\frac{D_{\mathrm{Clus}}}{D_{\mathrm{M31}}}\right)^{2} \backsimeq \frac{\Phi_{\mathrm{M31}}}{\Phi_{\mathrm{Dwarf}}} = \left(\frac{M_{M31}^{FOV}}{M_{\mathrm{Dwarf}}^{FOV}}\right)\left(\frac{D_{\mathrm{Dwarf}}}{D_{\mathrm{M31}}}\right)^{2} \gtrsim 1$$

XMM Study Results

For Ω_s = 0.24 & L = 0 density-production relationship [43]:

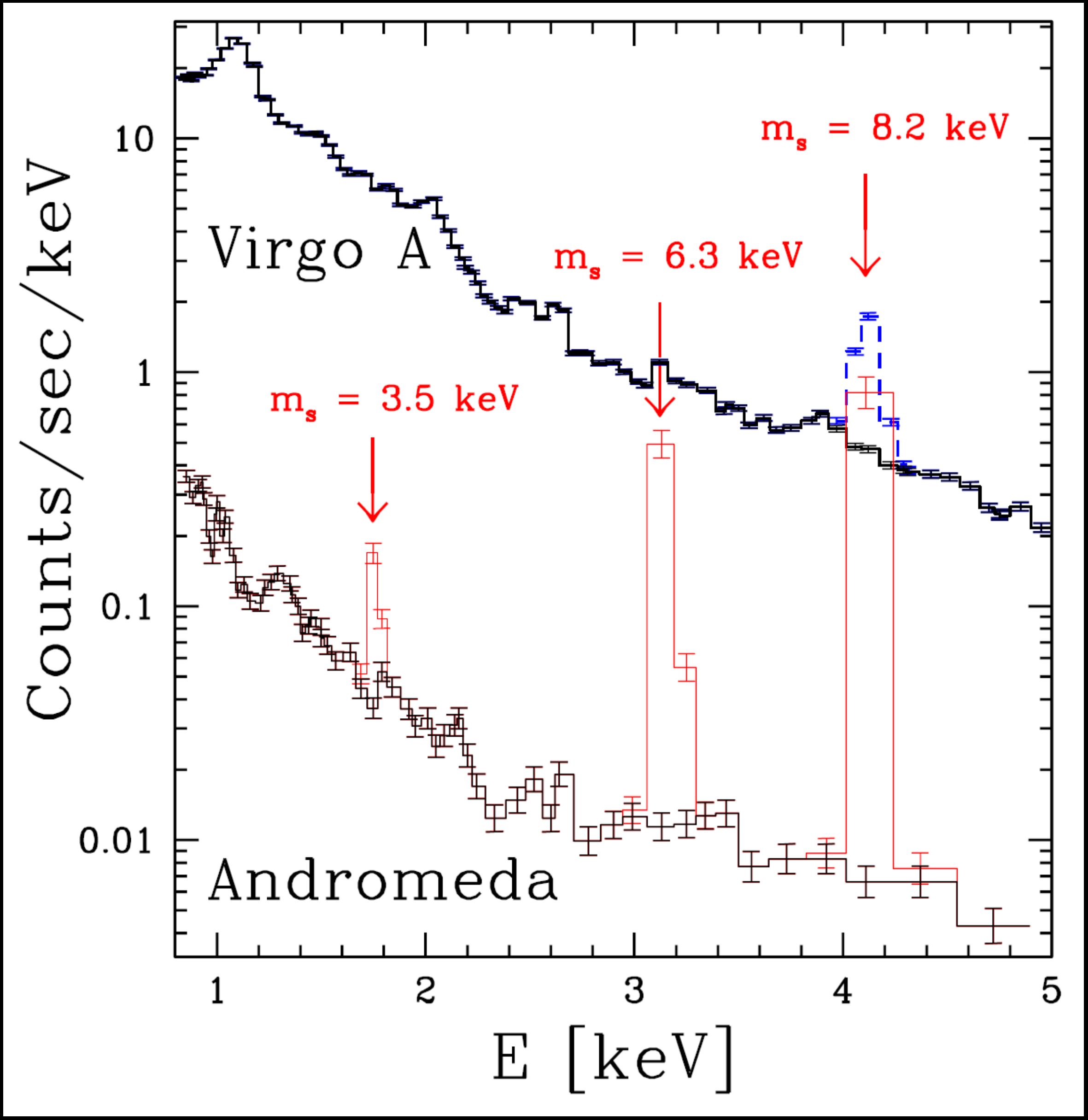

Andromeda:

m_s < 3.5 keV

[66]

Virgo A:

m_s < 8.2 keV

[44]

Virgo A+Coma:

m_s < 6.3 keV

[13, 63]

m_s = 6.3 keV & m_s = 8.2 keV decay peaks are also shown relative to Andromeda data.

Chandra FOV of M31: $\Delta\theta = 12' - 28'$

- Raw counts associated with the 7 Chandra ACIS-I exposure regions.

- Exposure times range from 5ks to 20ks

- Central 12' is excluded because of high astrophysical background from hot gas and point sources in that region

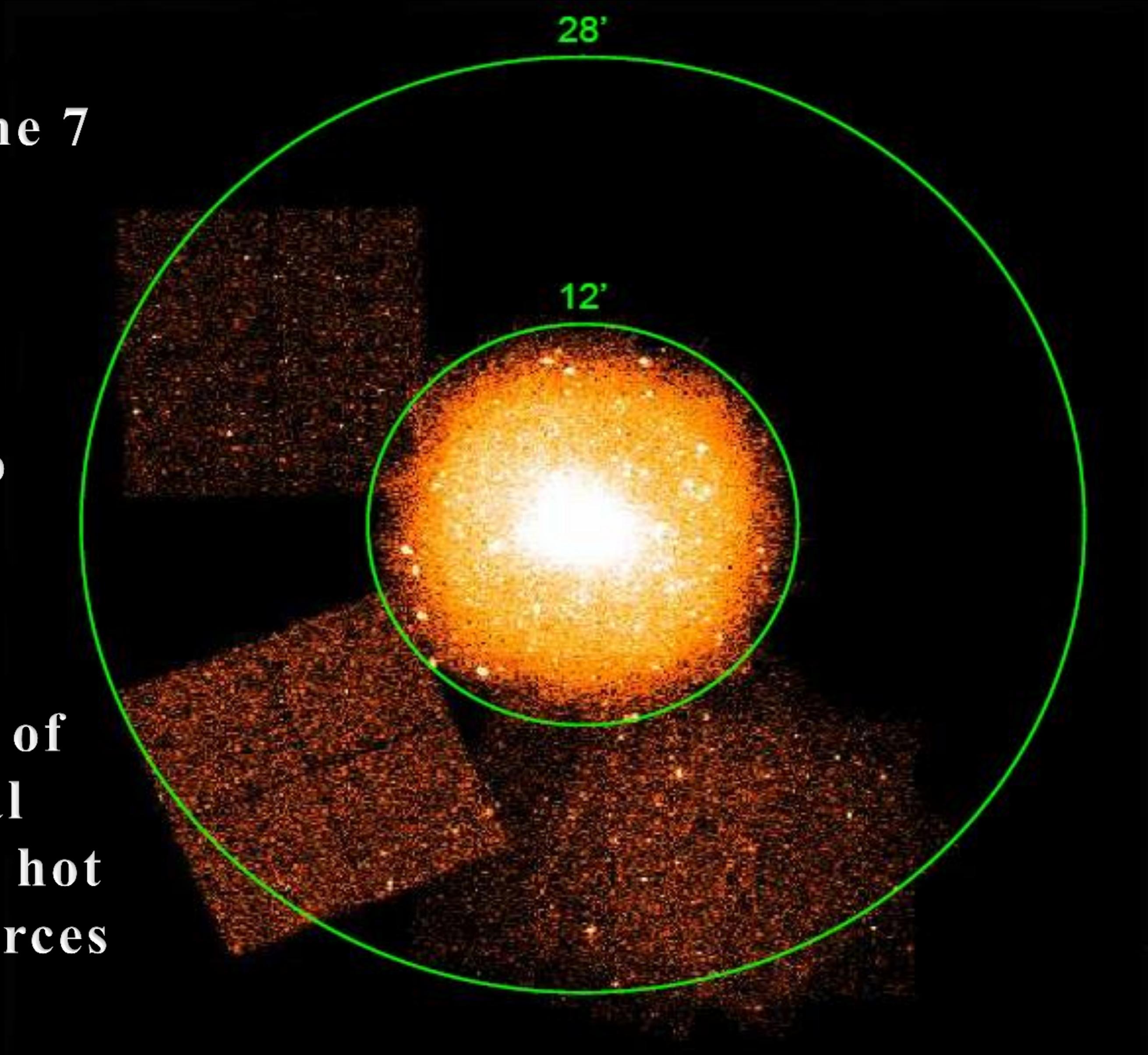

The Fraction of Andromeda's Dark Matter Mass in the *Chandra* field of view (FOV):

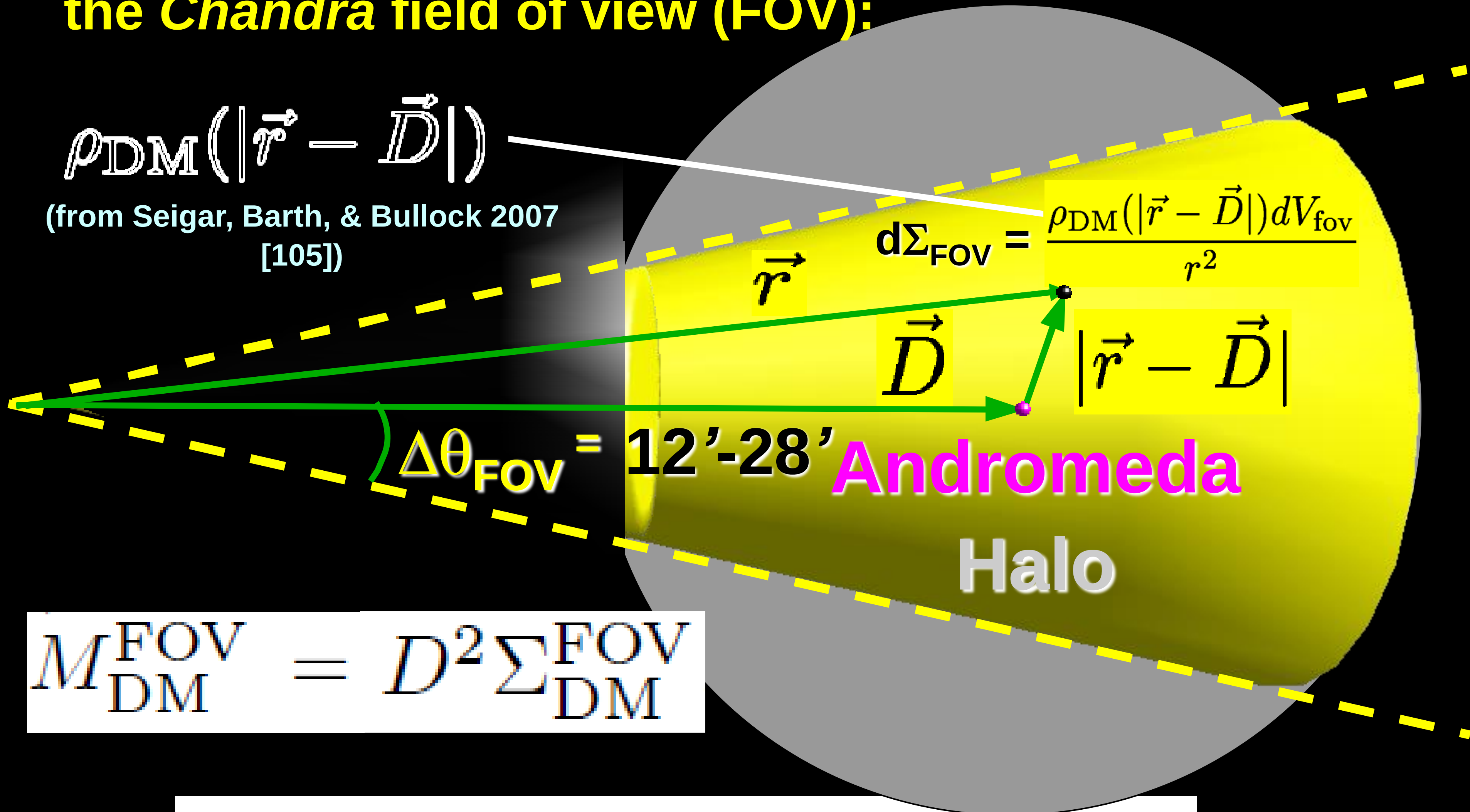

$$M_{\rm DM}^{\rm FOV} = D^2\Sigma_{\rm DM}^{\rm FOV}$$

$$\Sigma_{\rm DM,M31}^{\rm FOV} \simeq (0.8 \pm 0.04) \times 10^{11} M_\odot {\rm Mpc}^{-2}$$

$$M_{\rm DM,M31}^{\rm FOV} \simeq (0.49 \pm 0.05) \times 10^{11} M_\odot$$

Generalized constraints in the $m_s - \sin^2 2\theta$ plane

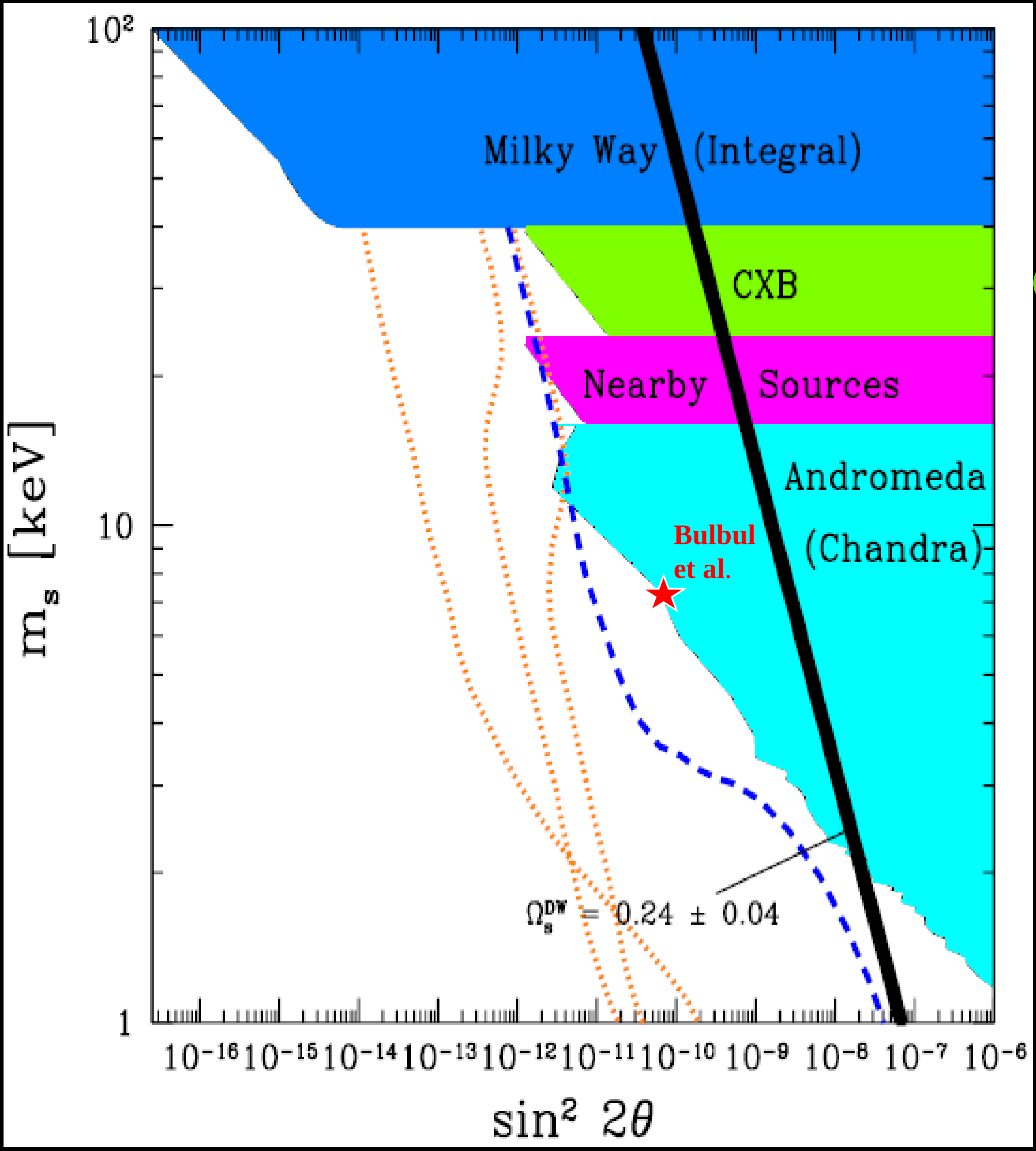

Exclusion Regions:

Milky Way (Integral):

[77, 78]

Cosmic X-ray Background:

[61,62]

Andromeda (XMM):

[66]

Andromeda (CXO):

(Watson, Li, & Polley 2012)

Density-Production Models:

Dodelson-Widrow Model

[3]

Shi-Fuller Model

[4, 53]

3 L >> 10^{-10} Lines

[13]

Dodelson-Widrow Excluded according to Horiuchi et al. (2014)

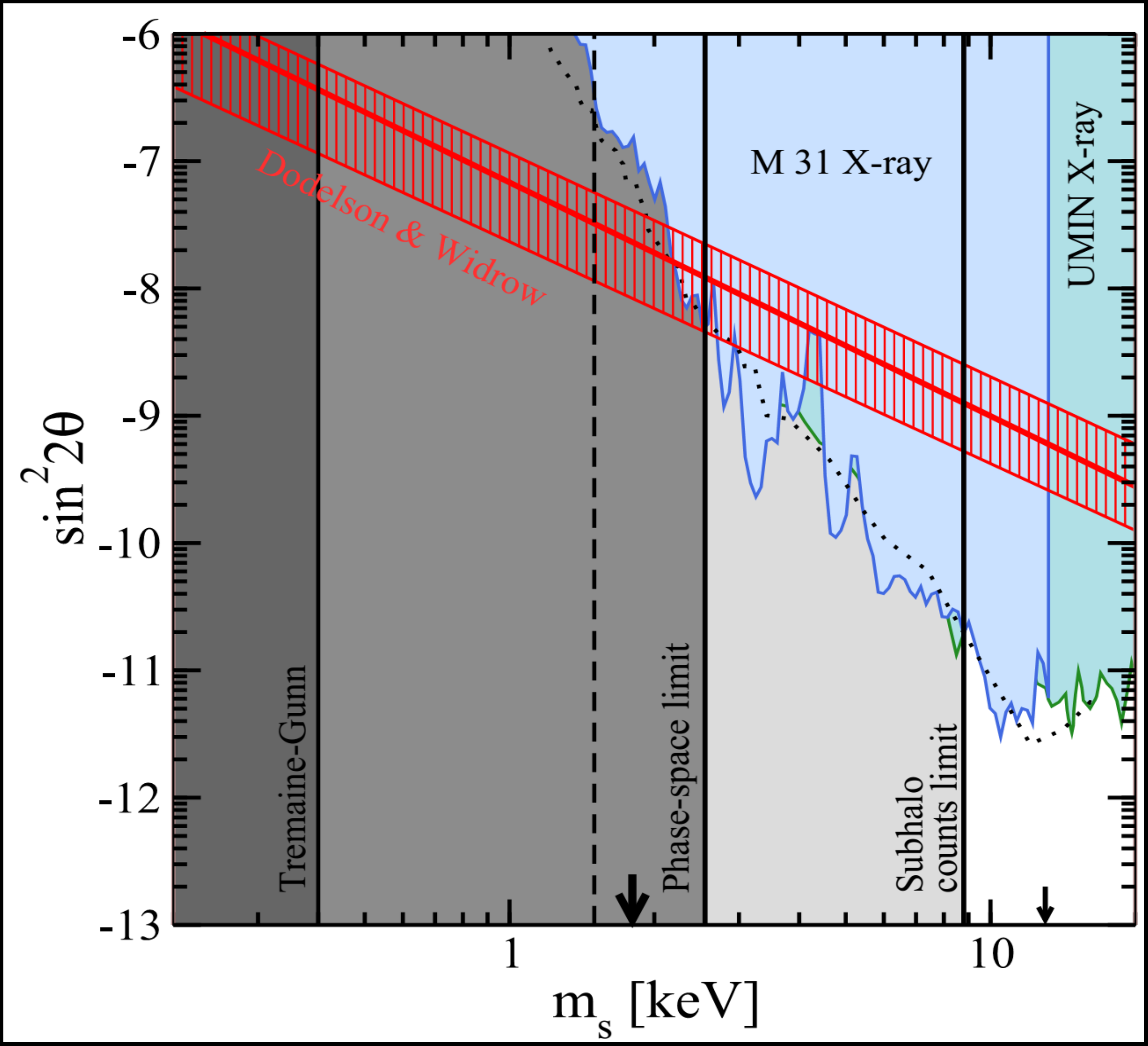

Bulbul et al. (2014):
Detection of An Unidentified Emission Line

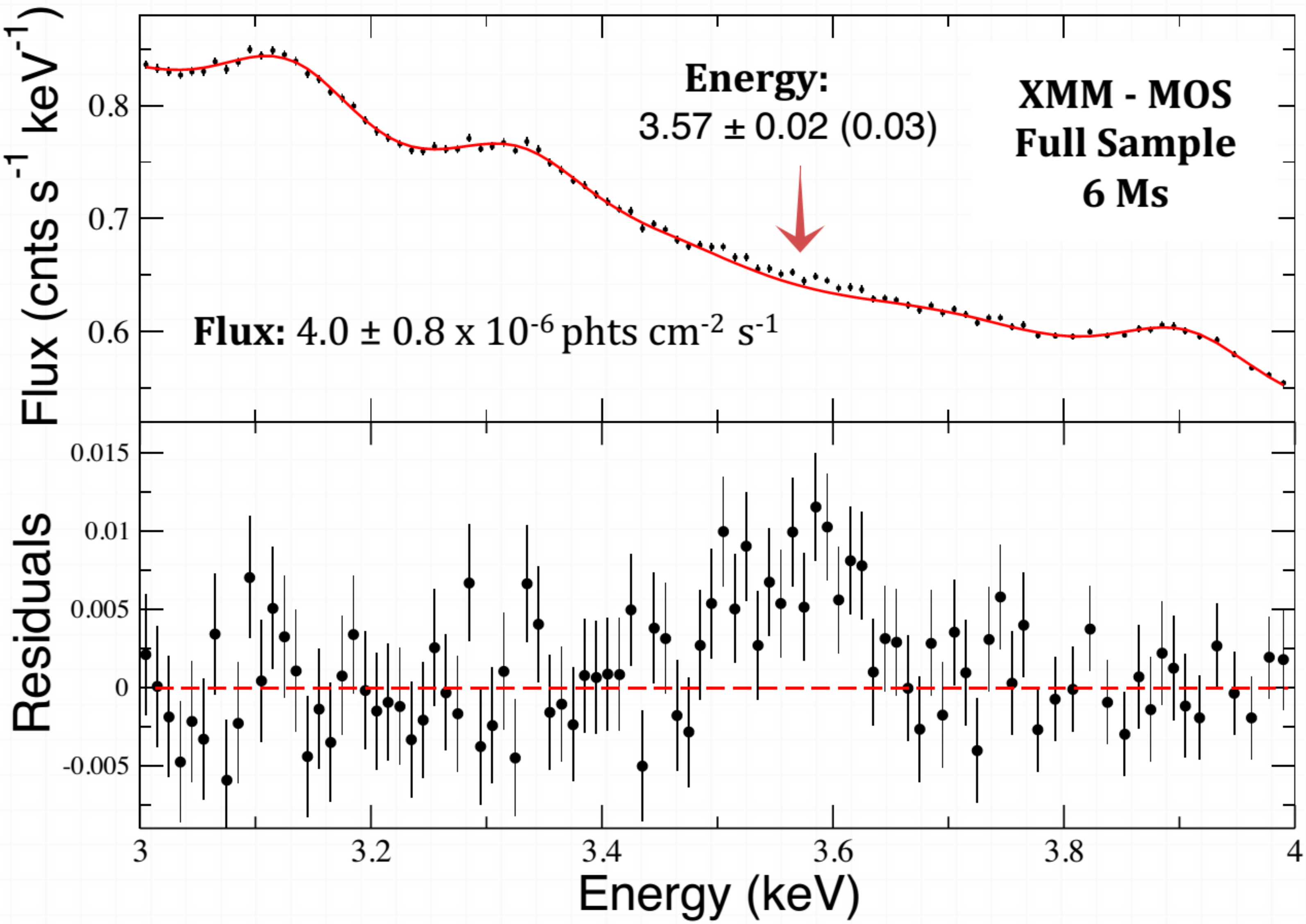

Possible Detection?

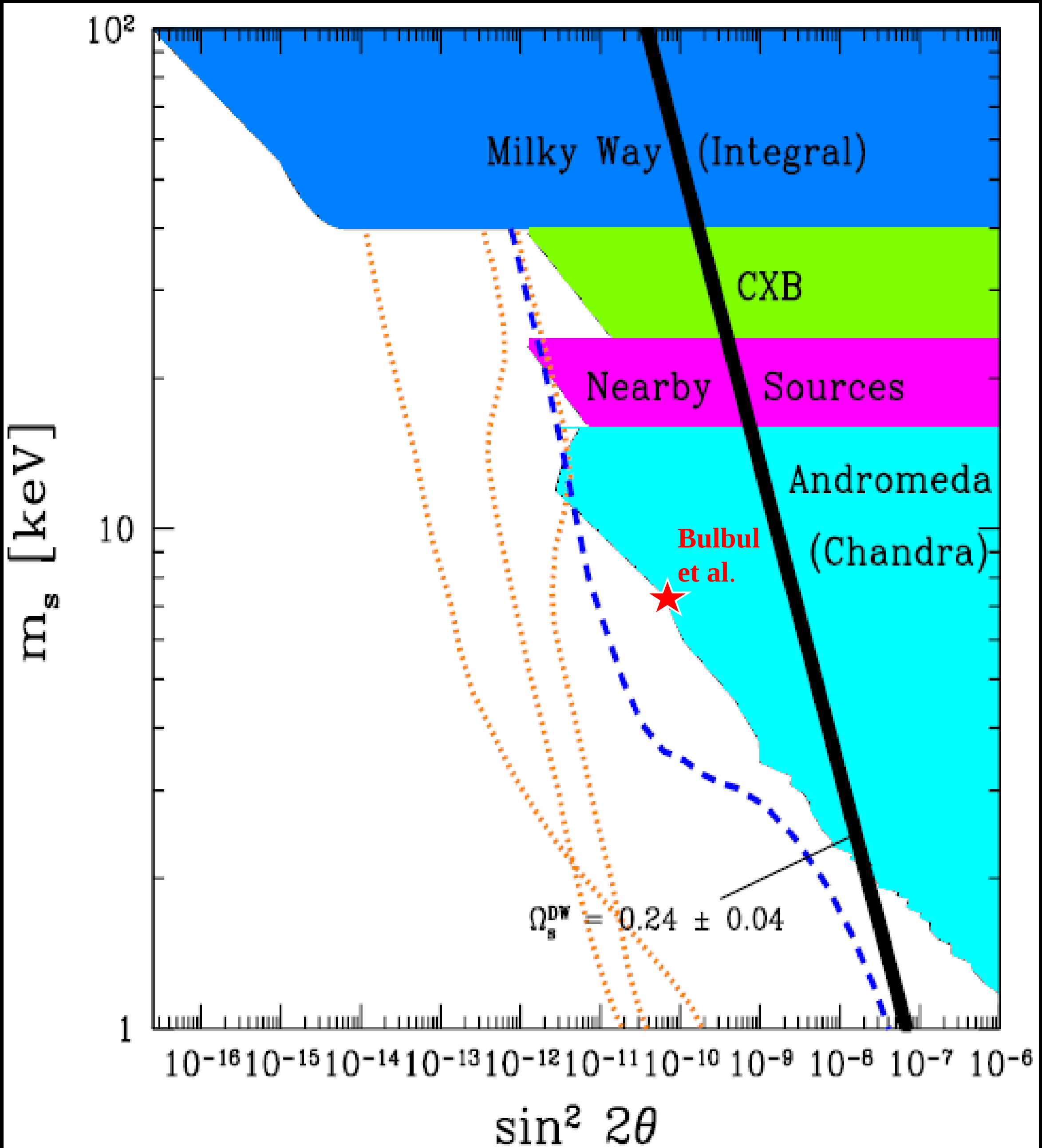

Bulbul et al. (2014):

$m_s = 7.14 \pm 0.1$ keV

$\sin^2 2\theta = 6.7 \pm 2.5 \times 10^{-11}$

- Not a background feature
- Not an instrumental line
- Not a detector feature
- Not a modeling artifact
- Comes from all clusters rather than a few dominant bright clusters
- Flux is centrally concentrated

On the cusp of exclusion:

Andromeda (CXO)

(Watson, Li, & Polley 2012)

(Horiuchi et al. 2014)

3.57 keV line avoids exclusion at lowest mixing (Horiuchi et al. 2014)

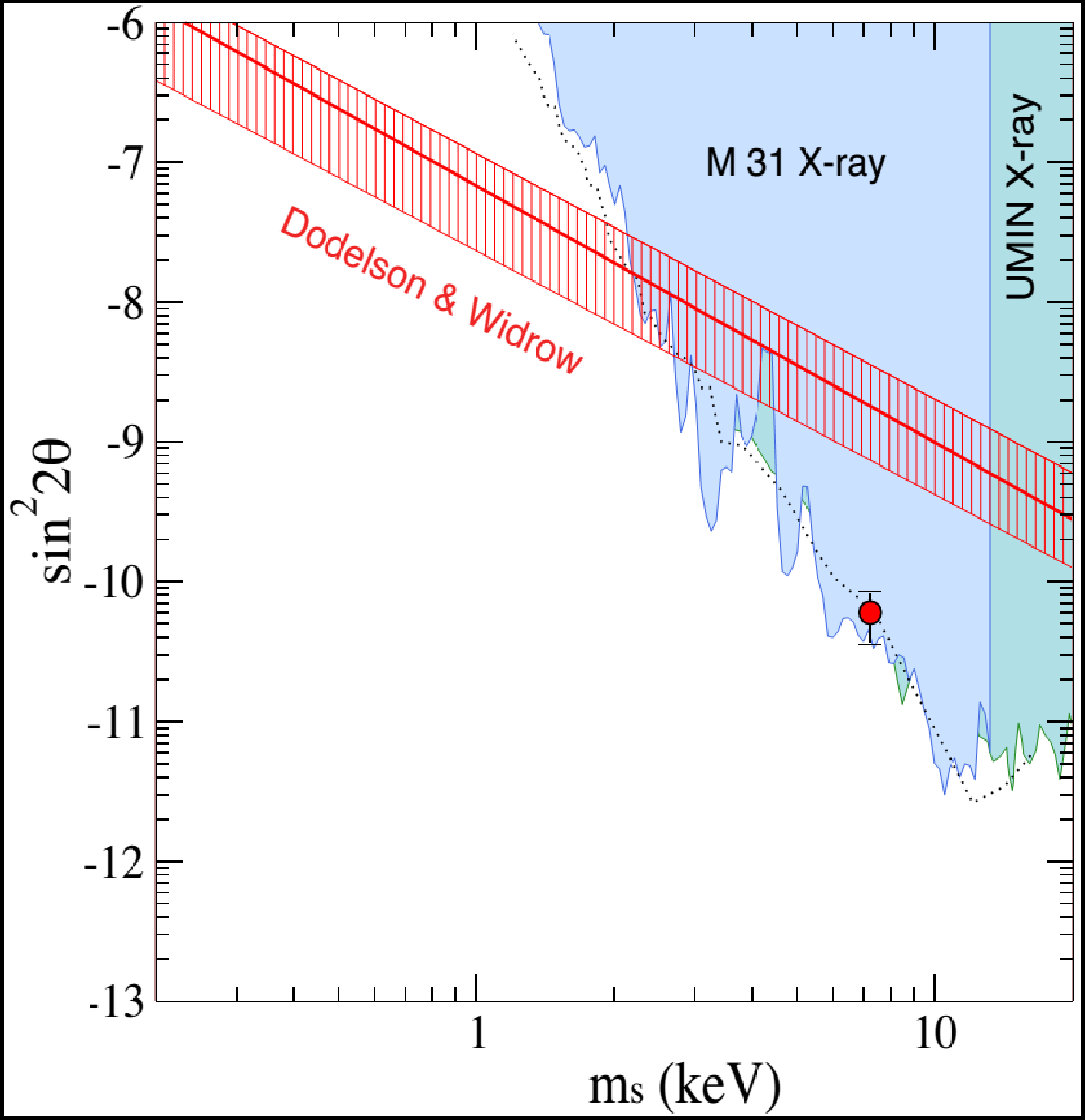

Bulbul et al. OK if:

$\sin^2 2\theta \simeq 3\text{-}4\times10^{-11}$

Andromeda (CXO) Exclusion Constraints:

Dotted (Watson, Li, & Polley 2012)

Solid (Horiuchi et al. 2014)

Shi-Fuller Models (Abazajian 2014)

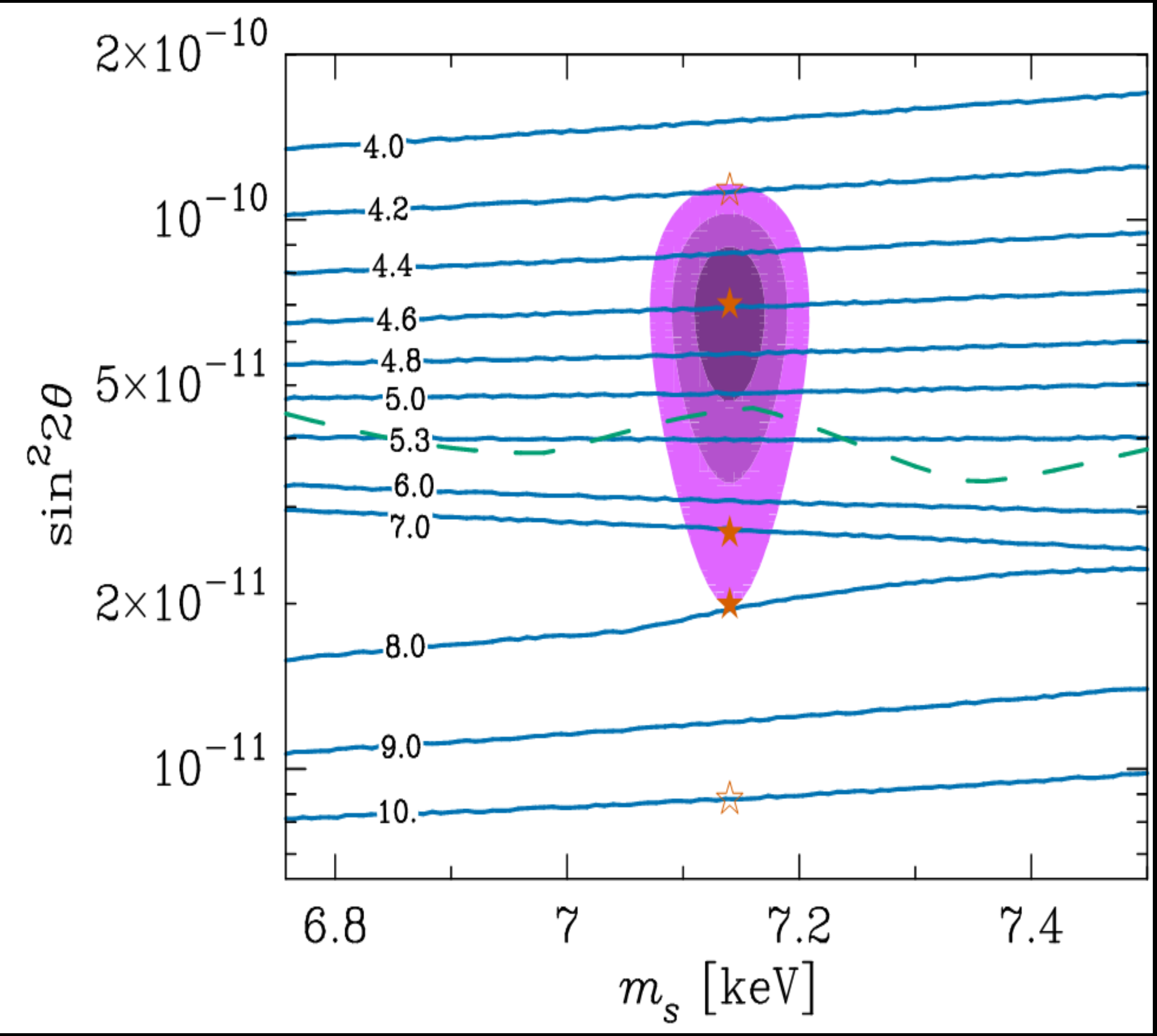

Bulbul et al.:

$m_s = 7.14 \pm 0.1$ keV

$\sin^2 2\theta \simeq 6.7\text{x}10^{-11}$

corresponds to

$L = 4.6\text{x}10^{-4}$,

i.e., $L_4 = 4.6$

IMPORTANT

Lower mixing:

$\sin^2 2\theta \simeq 3\text{x}10^{-11}$

corresponds to

$L_4 = 7.0$

ν_s Transfer Functions I: Shi-Fuller vs. Thermal (Abazajian 2014)

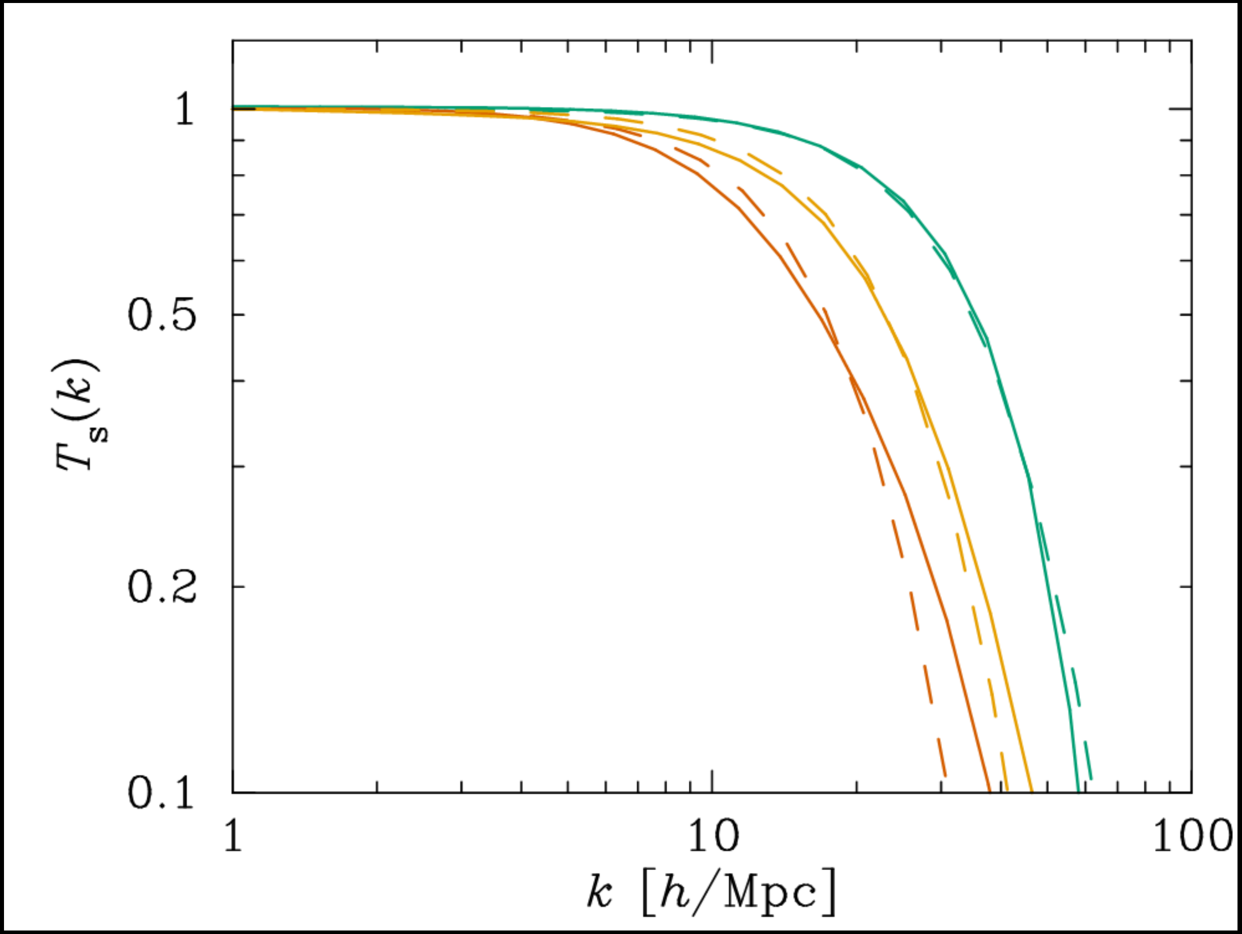

Solid

L_4 = 8, 7, 4.6

Dashed

m_{th}/keV = 1.6, 2.0, 2.9

Galaxy Constraints Satisfied by 2 keV Thermal Dark Matter Particle (Abazajian 2014)

- **Local Group Phase Space Density and Subhalo Counts:**
  m_{th} > 1.7 keV (Horiuchi et al. 2014)

- **High Redshift Galaxy Counts:**
  m_{th} > 1.3 keV (Schultz et al. 2014)

- **Abundance, Radial Distribution, and Inner Density Profile Crises of Milky Way Satellites solved if:**
  $m_{th} \simeq 2$ keV (e.g., Lovell et al. 2012 and Abazajian 2014 for additional references)

- **Recall that a 7.14 keV Shi-Fuller ν_s with $L_4 = 7$:**
  BEHAVES LIKE $m_{th} \simeq 2$ keV!

ν_s Transfer Functions II: Lyα Constraints

Scalar Decay, Shi-Fuller, DW (Merle & Schneider 2014)

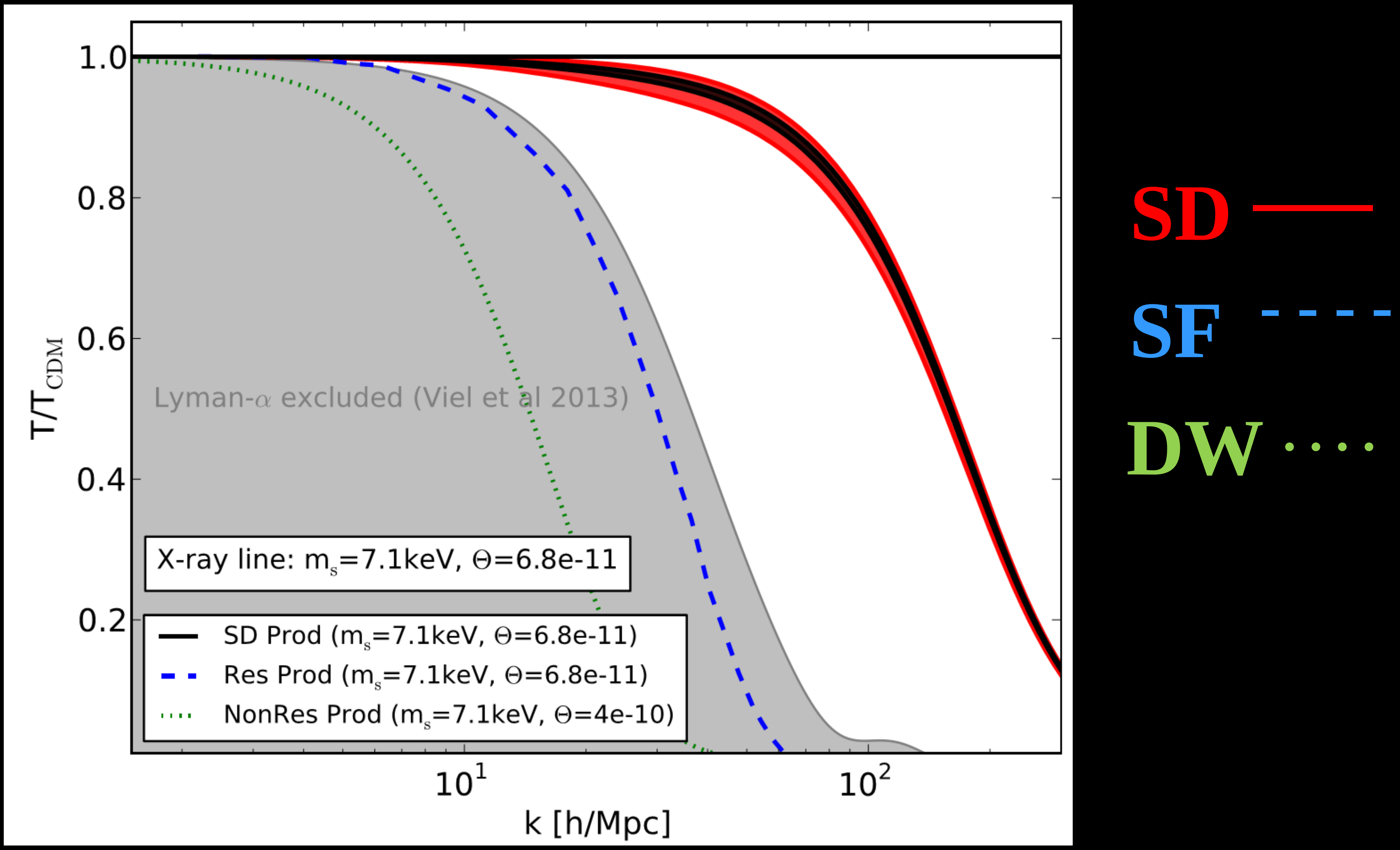

ν_s Halo Mass Function:

Scalar Decay, Shi-Fuller, DW (Merle & Schneider 2014)

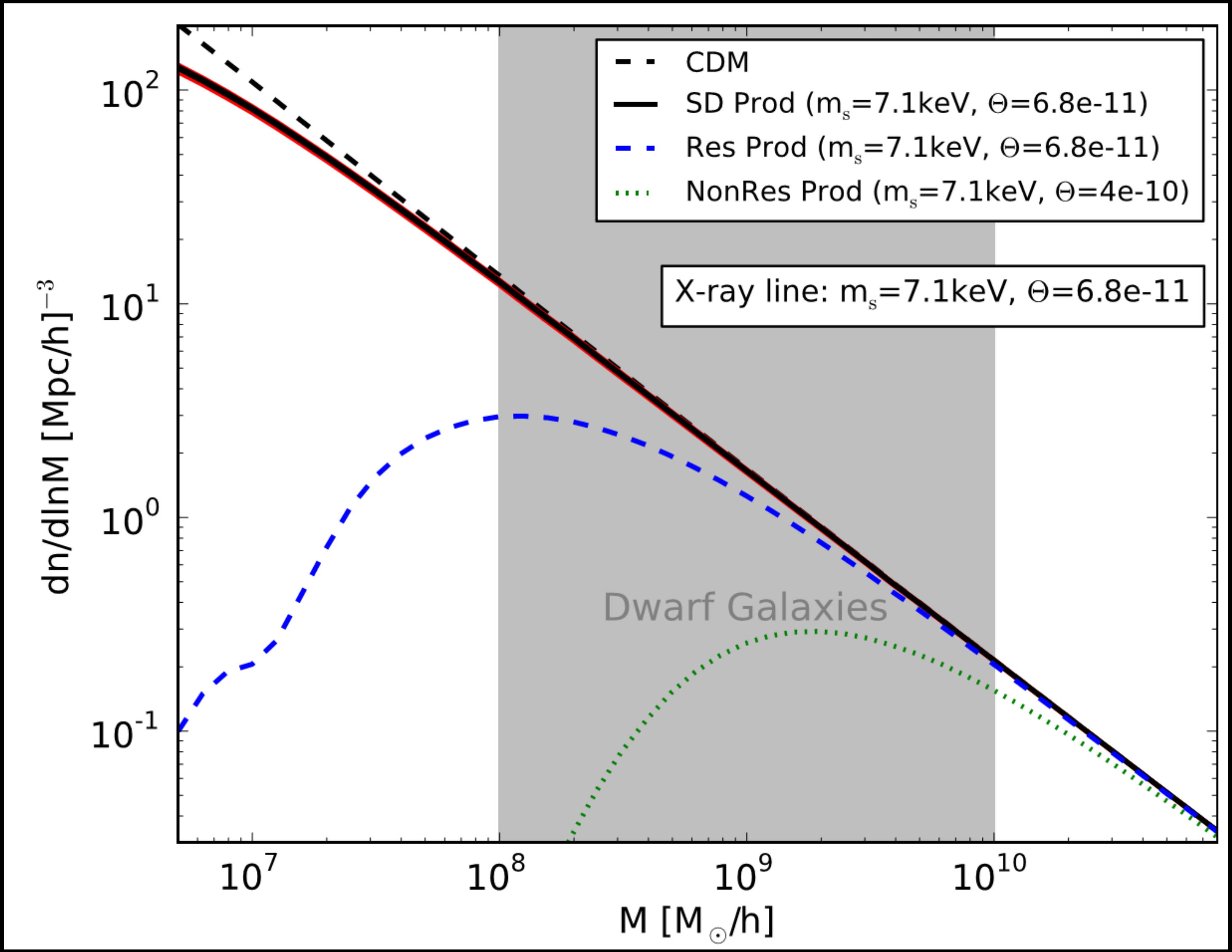

SD

SF

DW

Suzaku XRB observations do not exclude line (Sekiya et al. 2015)

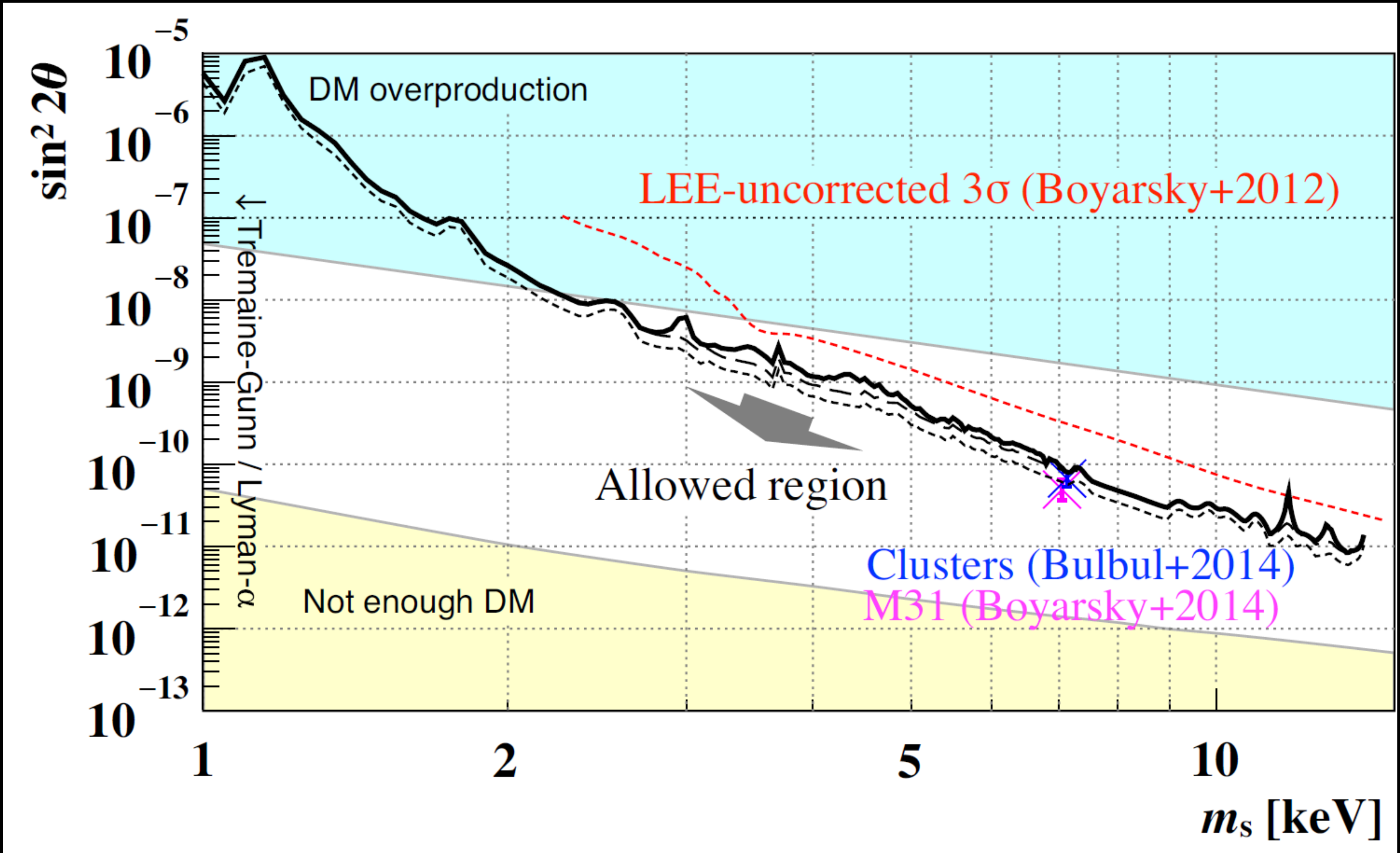

Avoids CMB/PSD exclusion in NEW Model (Lello & Boyanovsky 2015)

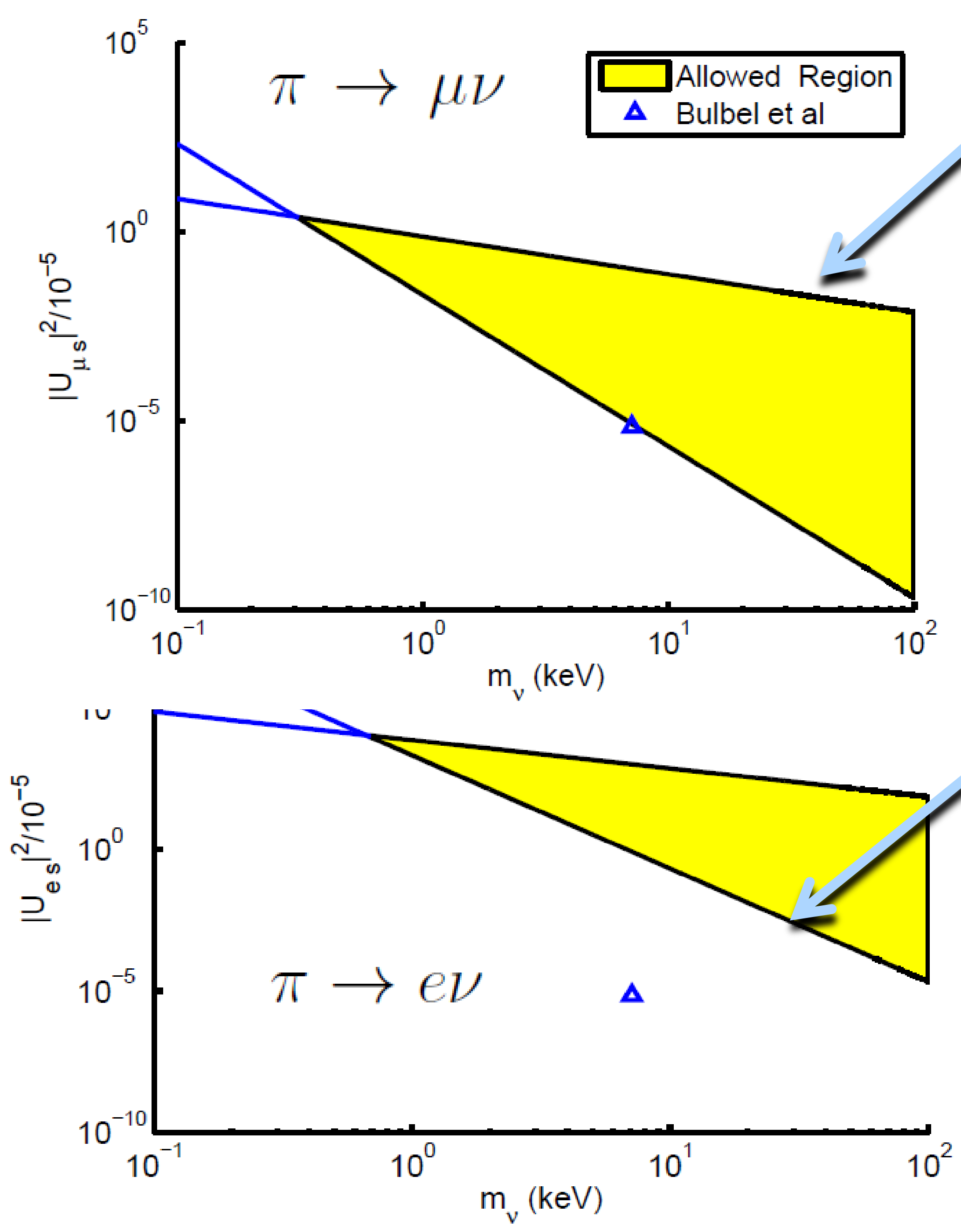

Upper bound: CMB (excess relativistic energy density)

$$m_{\nu_s}\,\frac{|U_{\mu s}|^2}{10^{-5}} \leq 0.739\,\mathrm{keV}$$

$$m_\nu \left(\frac{|U_{\mu s}|^2}{10^{-5}}\right)^{1/4} \geq 0.38\,\mathrm{keV}$$

Lower bound: PSD (Observed PSD less than primordial PSD)

$$m_{\nu_s}\,\frac{|U_{es}|^2}{10^{-5}} \leq 7242\,\mathrm{keV}$$

$$m_\nu \left(\frac{|U_{es}|^2}{10^{-5}}\right)^{1/4} \geq 6.77\,\mathrm{keV}$$

Observational Status of 3.57 keV line – Oct. 2014

Favored:

Boyarsky, et al. I (M31 + Perseus)

Abazajian, et al. (SF; Galaxy Observations)

Boyarsky, et al. II (MW + clusters)

Merle & Schneider (TFs + Lyα)

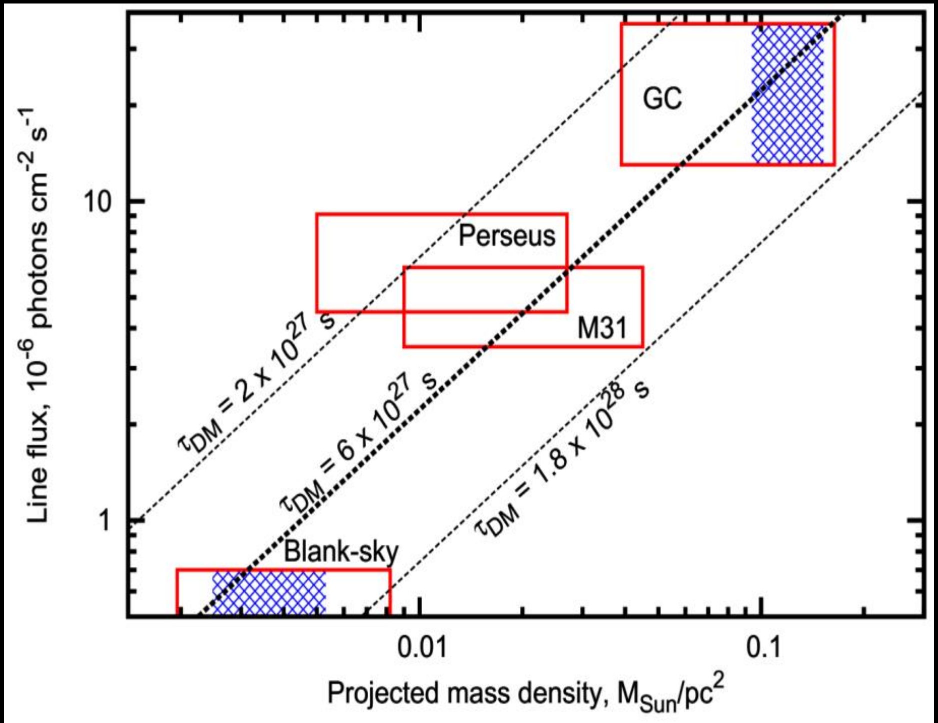

Fig. 2 of Boyarsky, et al. II

Disfavored:

Riemer-Sorensen (MW)

OK with "most conservative assumptions"

Exclusion after subtraction of "background emission lines".

Critique: Spectral model (Boyarsky, et al. II)

Jeltema & Profumo (MW, M31, Clusters)

Incorporating new K and Cl spectral lines, J&P find no evidence for 3.5 kev line.

Critiques: Spectral model (Notes from Boyarsky et al. and Bulbul et al.)

Malyshev et al. (MW dSphs)

Anderson et al. (Stacked Galaxies)

Both find no signal, BUT
Exclude central regions (of max DM density).
Lack of signal consistent with M31 outskirts.

Serious Problems I (Urban et al. 2015)

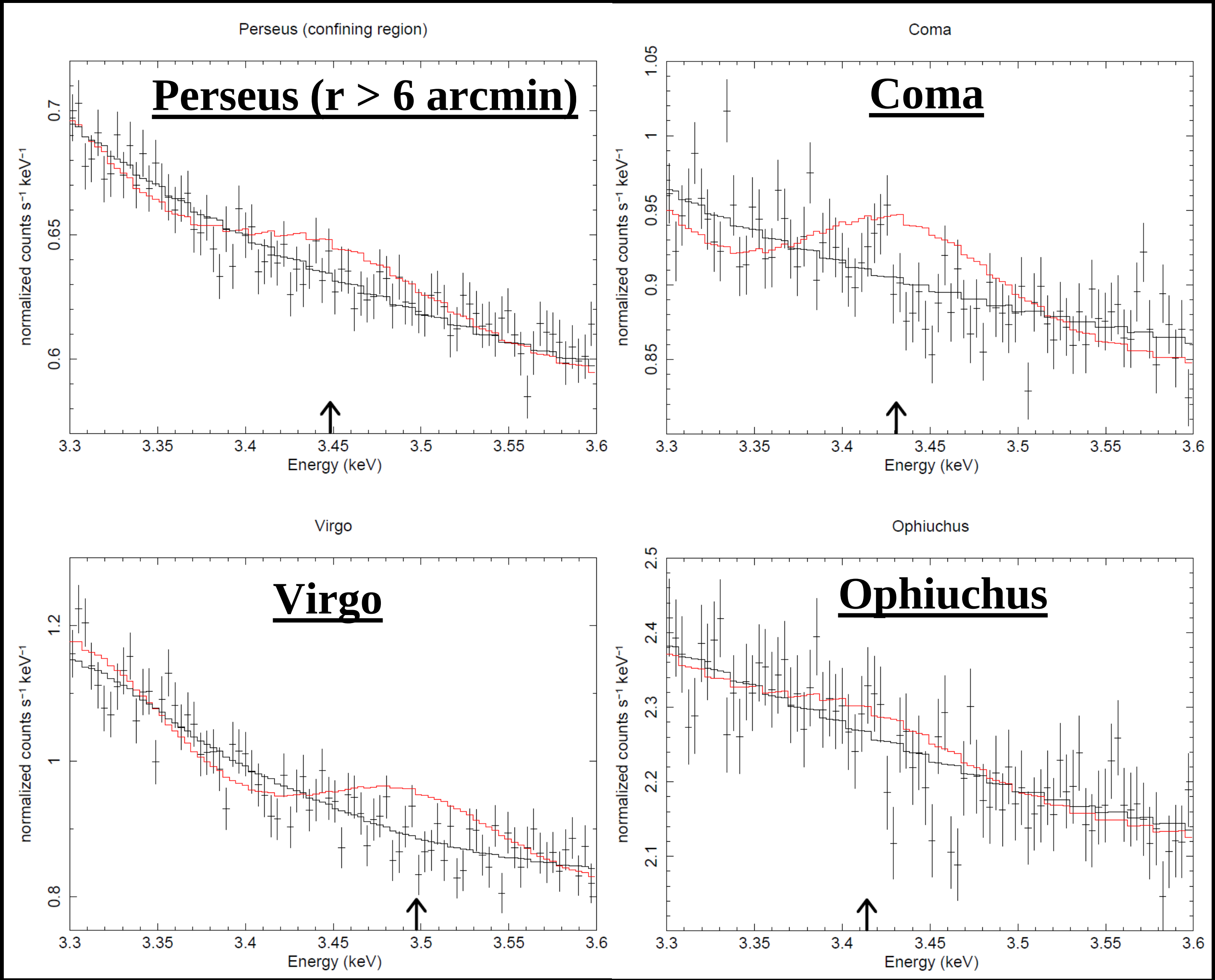

Find line in Perseus (r < 6')

If DM → red

Expect 50% core signal at r > 6'.

See < 10%.

Serious Problems II (Carlson et al. 2015)

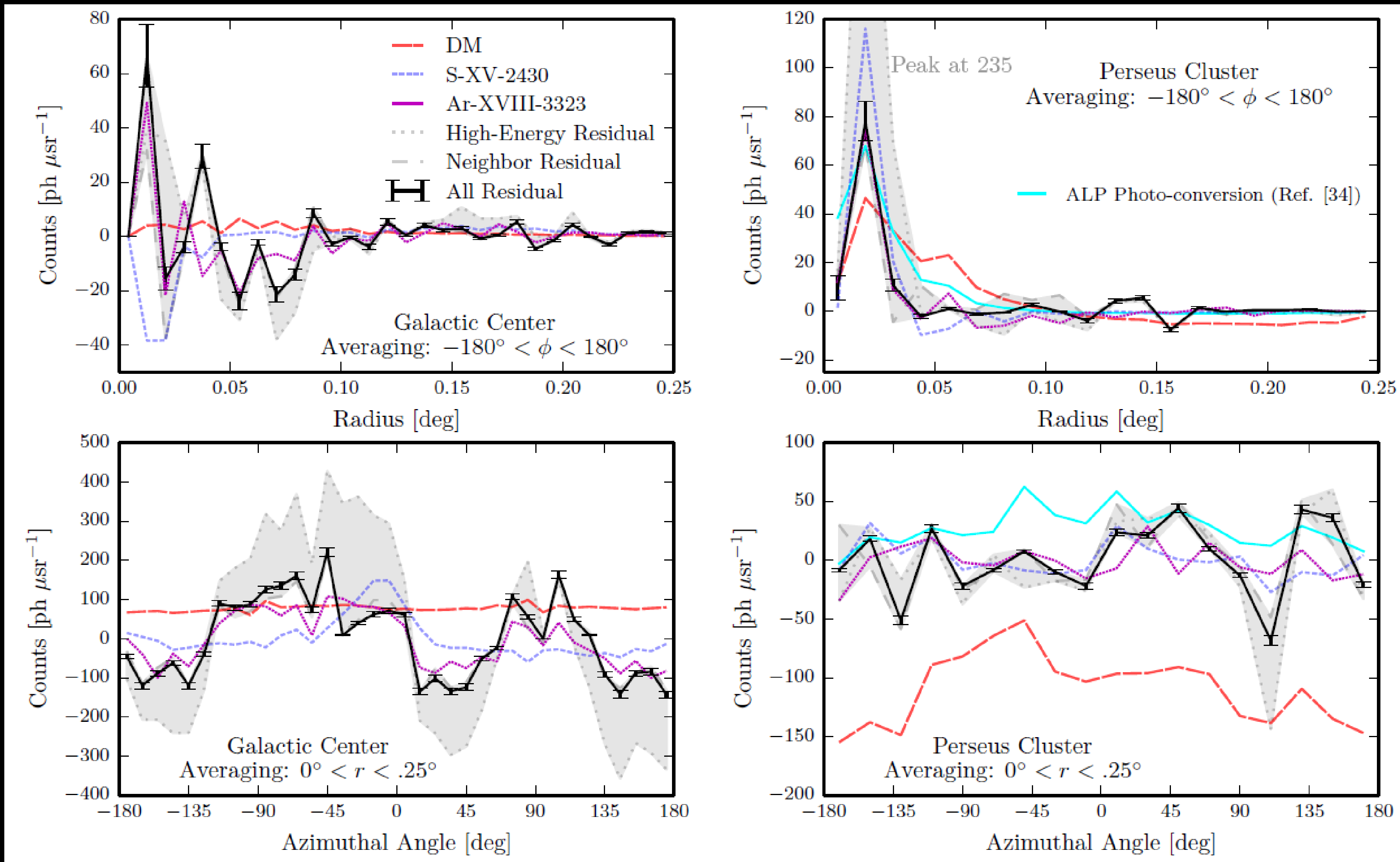

Galactic Center Perseus

Decaying DM *strongly disfavored* to explain full emission morphology

Summary I

DW excluded via phase space constraints from MW dwarfs.

(Horiuchi, et al. 2014)

A 7.14 keV Shi-Fuller sterile neutrino with $L_4 = 7$:

- Accounts for X-ray line anomaly found by Bulbul et al.
- Satisfies all galaxy constraints like $m_{th} \simeq 2$ keV
- Avoids exclusion by Andromeda X-ray Constraints
- Avoids exclusion by Lyα

(Abazajian, et al. 2014; Merle & Schneider 2014)

- **BUT appears to be ruled out due to emission morphology inconsistencies**

(Urban, et al. 2015; Carlson et al. 2015)

Part II:
More General DM Constraints via MW dSphs

- Phase Space Density
- Velocity Dispersion Data

Phase Space Density Overview I

$$Q \propto \frac{\rho}{\sigma^3}$$

- For a fermionic thermal relic, Hogan & Dalcanton (2001) find:

$$Q_{\mathrm{HD}} = \frac{\rho}{(3\sigma^2)^{3/2}} = AQ_* \left(\frac{m}{\mathrm{keV}}\right)^4$$

- where A = 5 x 10^{-4} and $Q_* = \frac{M_\odot / pc^3}{(\mathrm{km\ s^{-1}})^3}$
- adiabatic invariant
- strongly mass-dependent

Phase Space Density Overview II

- **Hogan & Dalcanton's assume a 1-D velocity disperson.**
- **As in Horiuchi et al. (2014), we assume MB:**

$$Q = \frac{\rho}{(2\pi\sigma^2)^{3/2}} \simeq 0.33 Q_{\rm HD}$$

$$Q_P = A Q_* \left(\frac{m}{\rm keV}\right)^4$$

- **where A = 1.65 x 10^{-4} and** $Q_* = \frac{M_\odot / pc^3}{(\rm km\ s^{-1})^3}$

Connecting the Past to the Present

- **Galaxy formation processes alter Q by an unknown factor Z:**

$$Z = \frac{Q_P}{Q_0}$$

- **De Vega & Sanchez (2010) explored a number of analytical methods to find Z, concluding that**
  - **$1 \leq Z \leq 10^4$, in agreement with simulations**
  - **the mass of a thermal relic DM particle is ~ keV:**

$$\frac{m_{\rm th}}{\rm keV} = \left(\frac{Q_p}{A}\right)^{1/4} = \left(\frac{ZQ_0}{A}\right)^{1/4} \simeq 1 - 10$$

PSD Goals

1. Determine Z directly from the dwarf galaxy data to produce a model-independent mapping between Q_p and Q_0.
2. Use this empirical Z factor to determine the DM particle mass – both for thermal and non-thermal relics.
3. Identify primordial dwarf galaxies – i.e., systems for which $Q_0 \simeq Q_P$.
4. Draw insights from these primordial objects about the formation and evolution of galaxies.

Dwarf Galaxy Data (Sample)

- Data for 23 dSphs from Walker et. al. (2009)

Dwarf	σ (km/s)			ρ (M_Θ pc^{-3})			r_{hf} (pc)			$M(r_{hf})$ (10^7 M_Θ)		
Carina	6.6	$\pm$	1.2	0.1	$\pm$	0.04	241	$\pm$	23	0.61	$\pm$	0.23
Draco	9.1	$\pm$	1.2	0.3	$\pm$	0.08	196	$\pm$	12	0.94	$\pm$	0.25
Fornax	11.7	$\pm$	0.9	0.042	$\pm$	0.007	668	$\pm$	34	5.3	$\pm$	0.9
Leo I	9.2	$\pm$	1.4	0.19	$\pm$	0.06	246	$\pm$	19	1.2	$\pm$	0.4
Leo II	6.6	$\pm$	0.7	0.26	$\pm$	0.06	151	$\pm$	17	0.38	$\pm$	0.09
Sculptor	9.2	$\pm$	1.1	0.17	$\pm$	0.05	260	$\pm$	39	1.3	$\pm$	0.4
Sextans	7.9	$\pm$	1.3	0.019	$\pm$	0.007	682	$\pm$	117	2.5	$\pm$	0.9
U Minor	9.5	$\pm$	1.2	0.16	$\pm$	0.04	280	$\pm$	15	1.5	$\pm$	0.4
C Ven I	7.6	$\pm$	0.4	0.025	$\pm$	0.003	564	$\pm$	36	1.9	$\pm$	0.2
U Ma II	6.7	$\pm$	1.4	0.32	$\pm$	0.14	140	$\pm$	25	0.36	$\pm$	0.16

Q – r_{hf} Power-Law Relation

- **The power-law relations from Walker et al. (2009):**

$$\rho \propto r_{hf}^{-1.6}; \sigma \propto r_{hf}^{0.2} \rightarrow \quad Q \propto \frac{\rho}{\sigma^3} \propto r_{hf}^{-2.2}.$$

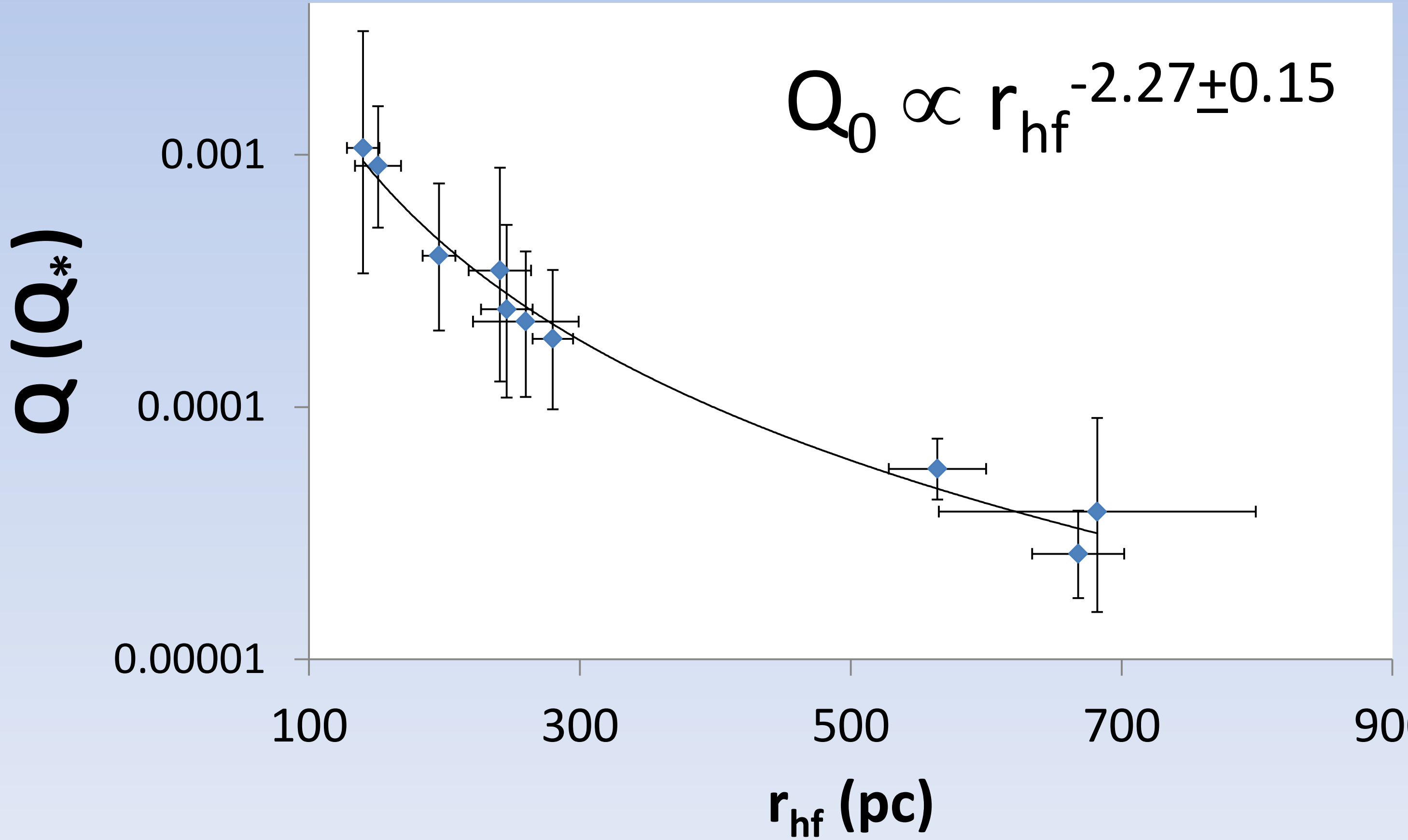

Phase Space Density of the DM

- Q_0 shown in the previous plot is based on *stellar* velocity dispersions, σ_*.
- Horiuchi et al. (2014) find

$$\eta_* = \sigma/\sigma_* = 1.5 \pm 0.2$$

- Adopting this correction factor, we find

$$Q_{0,\mathrm{DM}} = (1.61 \pm 0.42) Q_* \left(\frac{r_{hf}}{\mathrm{pc}} \right)^{-n}$$

- where $n = 2.27 \pm 0.15$ and $Q_* = \frac{M_\odot / pc^3}{(\mathrm{km\ s^{-1}})^3}$

Using $Q(r_{hf})$ to find Z

- We can rewrite the $Q(r_{hf})$ power-law in terms of:
  - the unknown, primordial Q_p

  and

  - an unknown radial scale, r_p:

$$Q_0 = Q_P \left(\frac{r_p}{r_{hf}} \right)^n = Q_P / Z_{\mathrm{em}}$$

$$Z_{\mathrm{em}} = (r_{hf}/r_p)^n$$

- Thus, determining r_p is the key to the empirical Z factor.

Empirical Upper Limits on r_P

Q can only decrease (Liouville's Theorem), so

$$Z = (r_{hf}/r_p)^n \geq 1$$

$$r_p \leq r_{hf,min}$$

<u>Minimum r_{hf} values:</u>

- **Willman 1: $r_{hf} = 25 \pm 6$ pc**
- **Segue 1: $r_{hf} = 29 \pm 7$ pc**
- **Segue 2: $r_{hf} = 34 \pm 5$ pc**

$$r_p \leq 19 - 39 \text{ pc}$$

Analytical Limit on r_p

- If r_p is the initial collapse analog of the contemporary half-light radius and
- At collapse the overdensity is well-characterized by an isothermal density profile,

$$M_{hf} \approx \frac{4}{3}\pi\rho_{m,0}\Delta\left(\frac{R_{vir}}{r_p}\right)^2 (1+z_c)^3 r_p^3$$

- For
  - $z_c \sim 10\text{-}15$
  - $R_{vir} \sim 1\text{-}2$ kpc
  - $r_p \sim 15 – 35$ pc

which coincides with empirical upper bounds.

Q_p + DM Particle Mass with $r_p = 25 \pm 10$ pc

- **Max/Min Q_0 ratio is ~ 10^4**
- **Max/Min Q_p differ by ~ 4.5**

$$Q_P = Z_{em} Q_0$$

- **Max/Min m_{th} values differ by ~ 1.5**

$$\frac{m_{\rm th}}{\rm keV} = \left(\frac{Z_{\rm em} Q_0}{A}\right)^{1/4} = \left(\frac{\left(\frac{r_{hf}}{r_p}\right)^n Q_0}{A}\right)^{1/4}$$

Including all galaxy data uncertainties

- **$1 < Z < 10^4$**
- **$0.74 < m_{th}/\text{keV} < 3.4$ (mean 1.55 keV)**

Non-thermal DM

- **If the DM particle is a sterile neutrino, we can use the following transformation equations (e.g., Viel et al. 2005; Abazajian 2014) to find the corresponding non-thermal limits:**

$$m_{s,\mathrm{DW}} = 4.27\mathrm{keV}\left(\frac{\mathrm{m_{th}}}{\mathrm{keV}}\right)^{4/3}\left(\frac{\Omega_{\mathrm{m,0}}\mathrm{h}^2}{0.1371}\right)^{-1/3} \simeq 1.5 m_{s,\mathrm{SF}}$$

- **Applying these transformations, we find:**

2.9 < m/keV < 22.1 (Dodelson-Widrow) X (Watson et al. 2012)

1.9 < m/keV < 14.7 (Shi-Fuller) X Bulbul et al. (2014) OK

- **Alternative transformations (deVega & Sanchez 2013):**

$$m_{\nu}^{\mathrm{DW}} = 2.85\mathrm{keV}\left(\frac{m_{\mathrm{th}}}{\mathrm{keV}}\right)^{4/3}; m_{\nu}^{\mathrm{SF}} \cong 2.55 m_{th}$$

1.9 < m/keV < 14.7 (Dodelson-Widrow) X (Horiuchi et al. 2014)

1.9 < m/keV < 8.6 (Shi-Fuller) X Bulbul et al. (2014) OK

Summary II

- **Using data from Walker et. al. (2009), we found a strong correlation between Q and r_{hf} for Milky Way dwarf satellite galaxies.**

- **Determing the primordial radial scale r_p, we established Q_P and limits on the DM particle mass:**
  - **$0.74 < m_{th}/\mathrm{keV} < 3.4$ (mean 1.55 keV)**
  - **DW ruled out, Shi-Fuller $1.9 < m_{SF}/\mathrm{keV} < 14.7$**

- **Comparing to Q_P, we see 3 *possibly* primordial MW dSphs: Segue 1, Segue 2, and Willman 1.**

Part II:
More General DM Constraints via MW dSphs

- **Phase Space Density**
- **Velocity Dispersion Data**

MW dSphs Velocity Dispersions (Gerringer-Sameth et al. 2015)

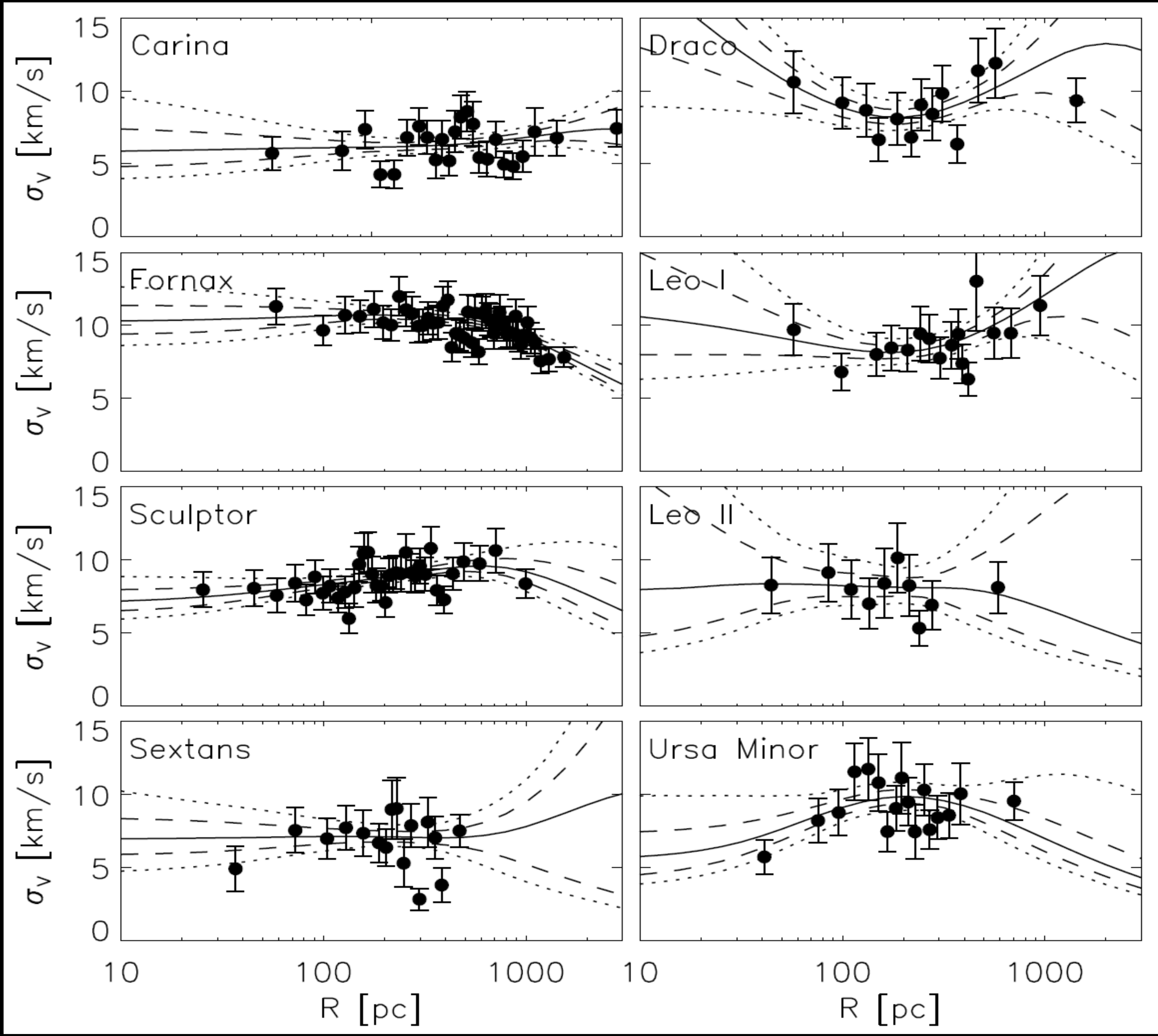

MW dSphs Velocity Dispersions (Gerringer-Sameth et al. 2015)

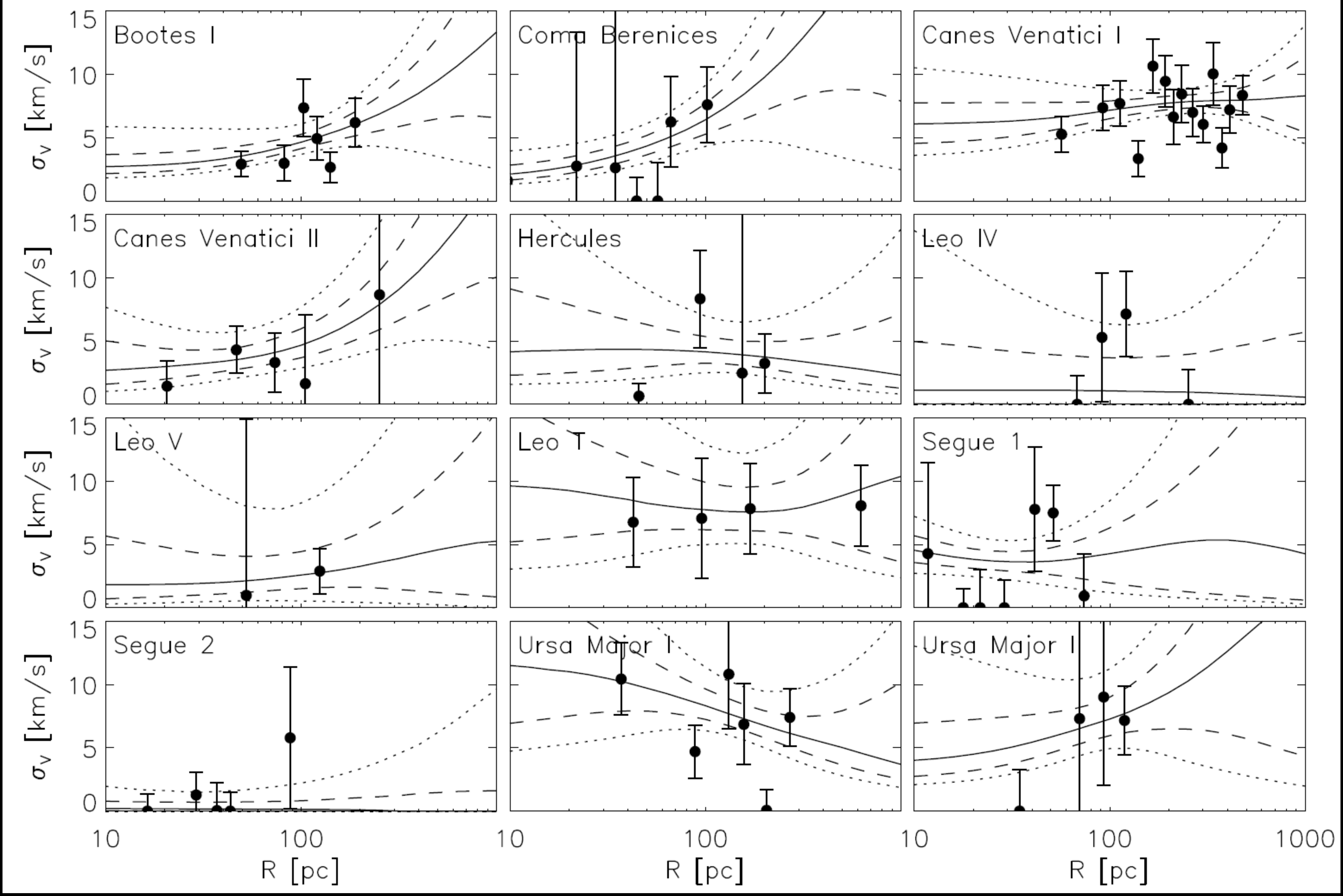

MW dSphs Velocity Dispersions (Gerringer-Sameth et al. 2015)

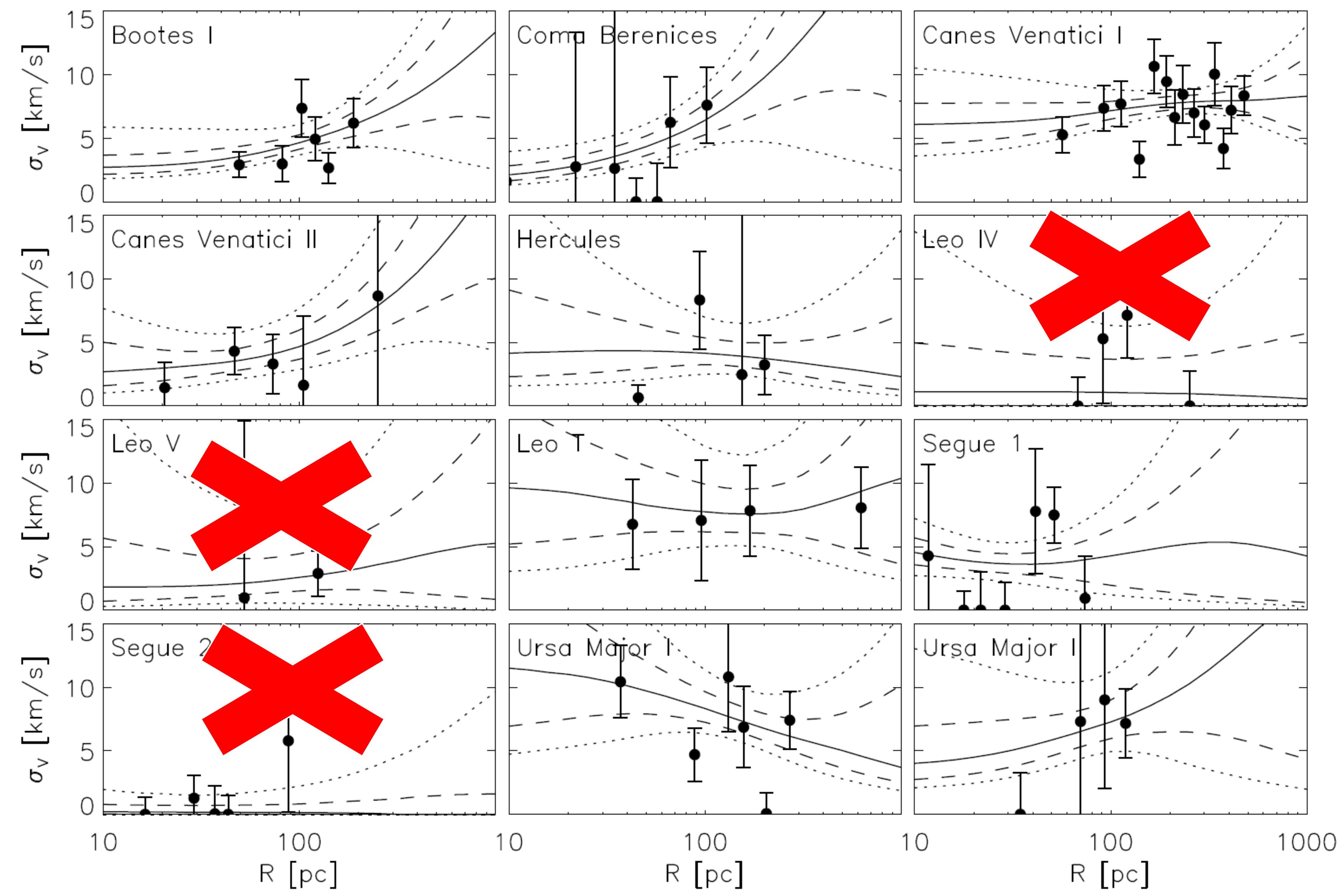

Best-Fit Burkert Mass Profiles

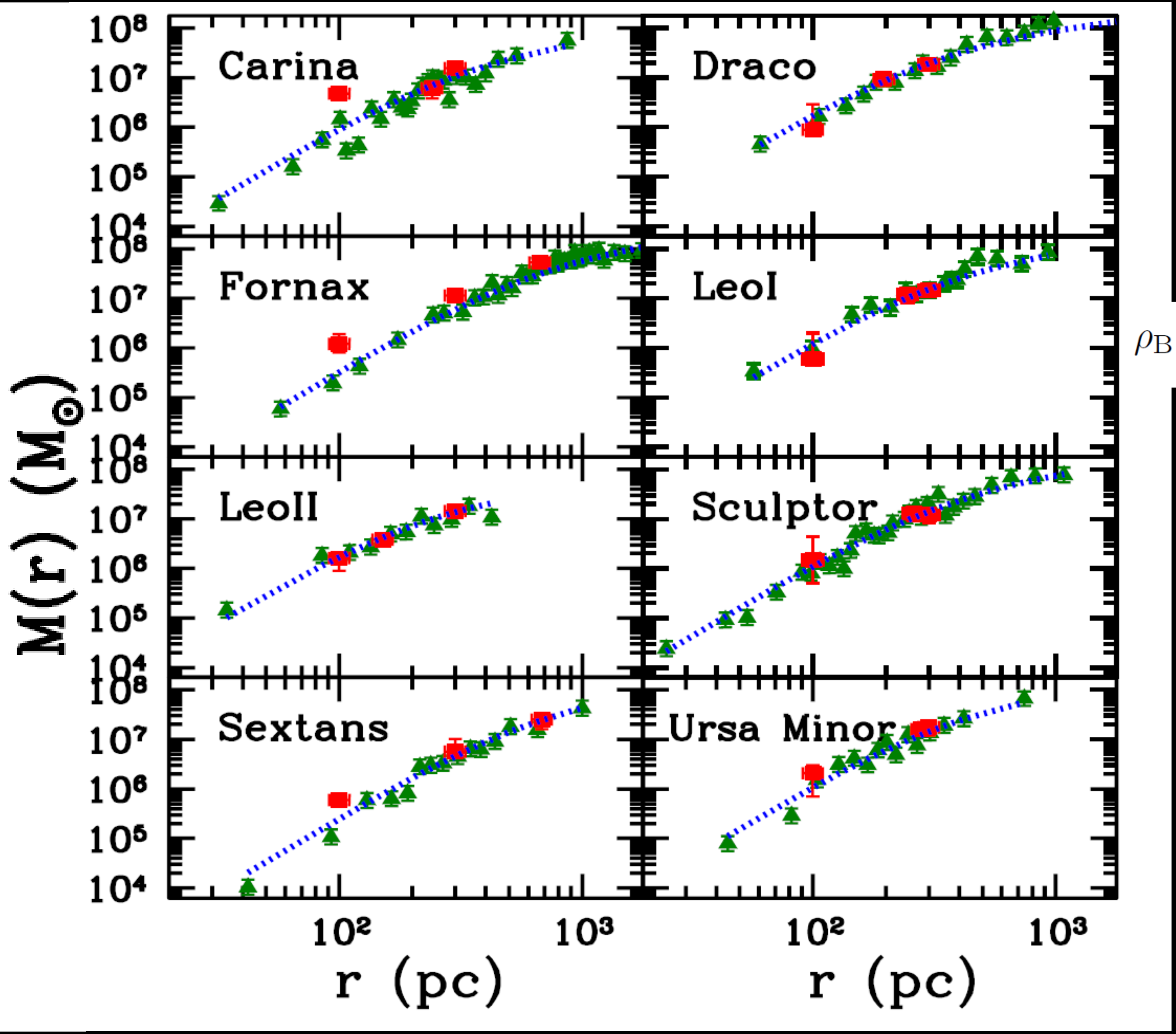

Best-Fit Burkert Profiles

$$\rho_B(r) = \frac{\rho_0}{(1+x)(1+x^2)},$$

where $x = r/r_0$

Strigari et al. (2009)

Walker et al. (2009) Data

The $r_0 - r_{hf}$ Correlation:

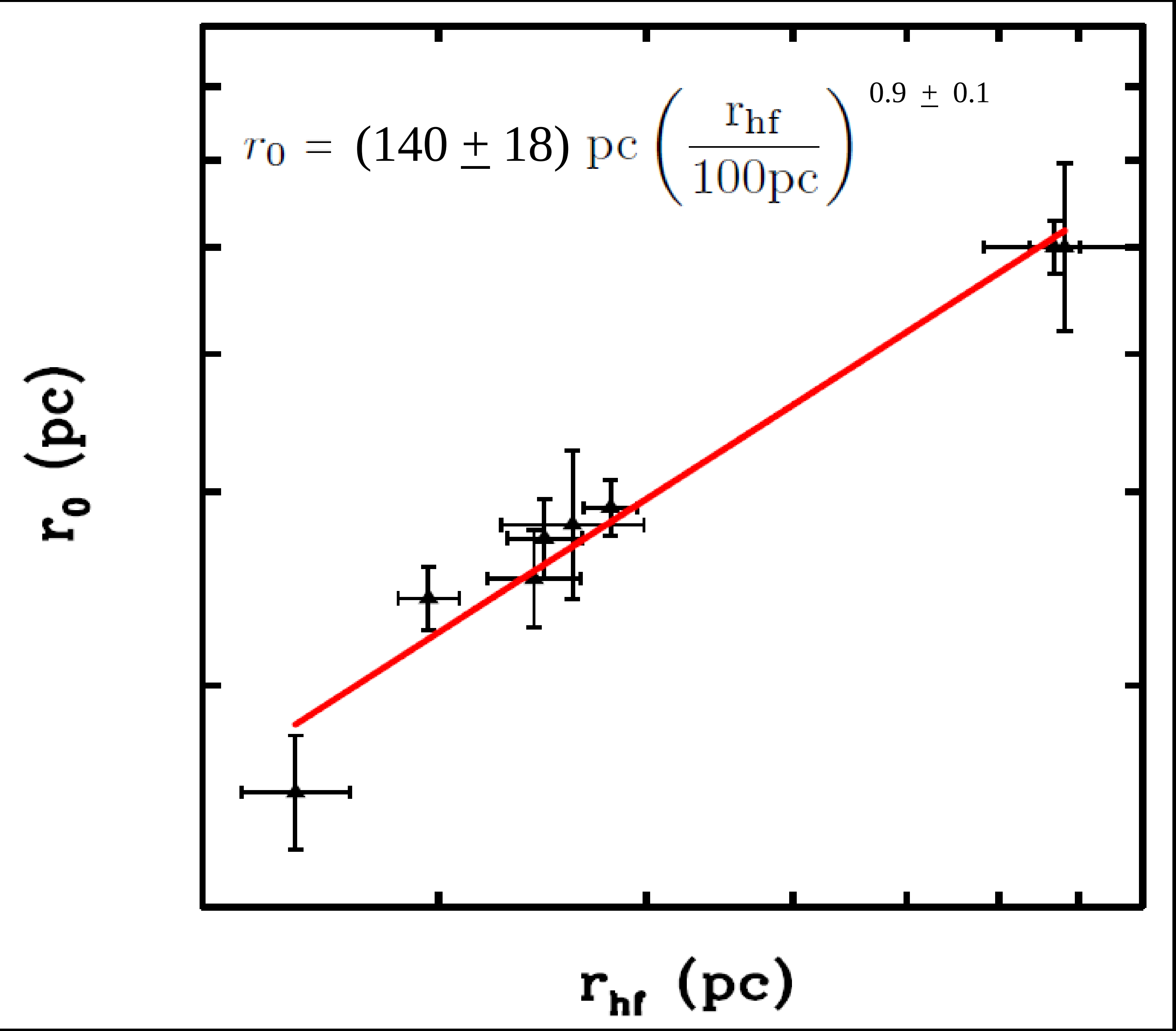

The $\rho_0 - r_{hf}$ Correlation:

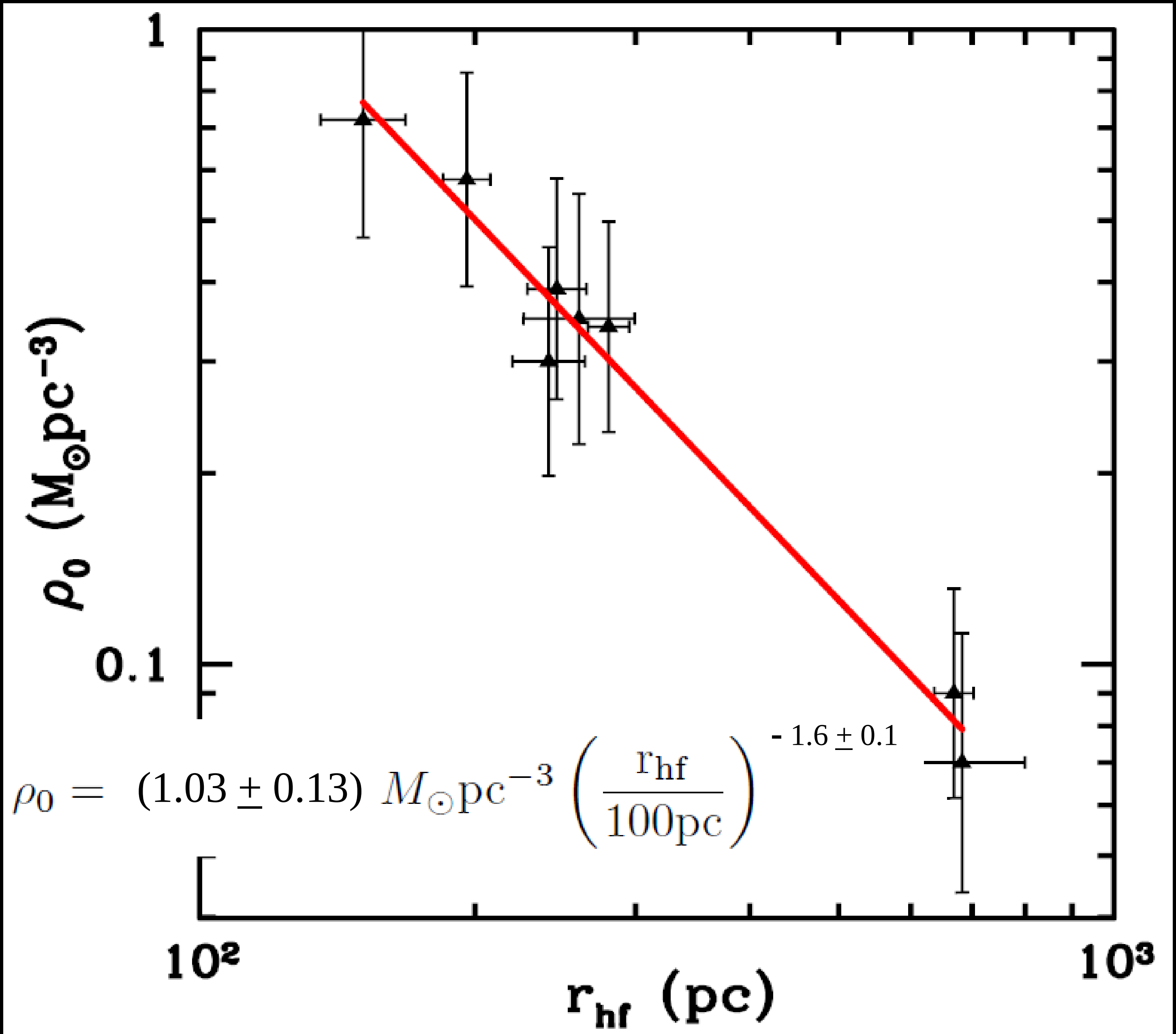

$$\rho_0 = (1.03 \pm 0.13)\ M_\odot \mathrm{pc}^{-3} \left(\frac{r_{hf}}{100\mathrm{pc}}\right)^{-1.6 \pm 0.1}$$

The $M_{hf} – r_{hf}$ Correlation Test:

$$M_B(r) = 4\pi \int_0^r s^2 \rho_B(s) ds$$

$$M(r_{hf}) = (5.0 \pm 1.3) \times 10^3 \, M_\odot \, (r_{hf}/\mathrm{pc})^{1.3 \pm 0.1}$$

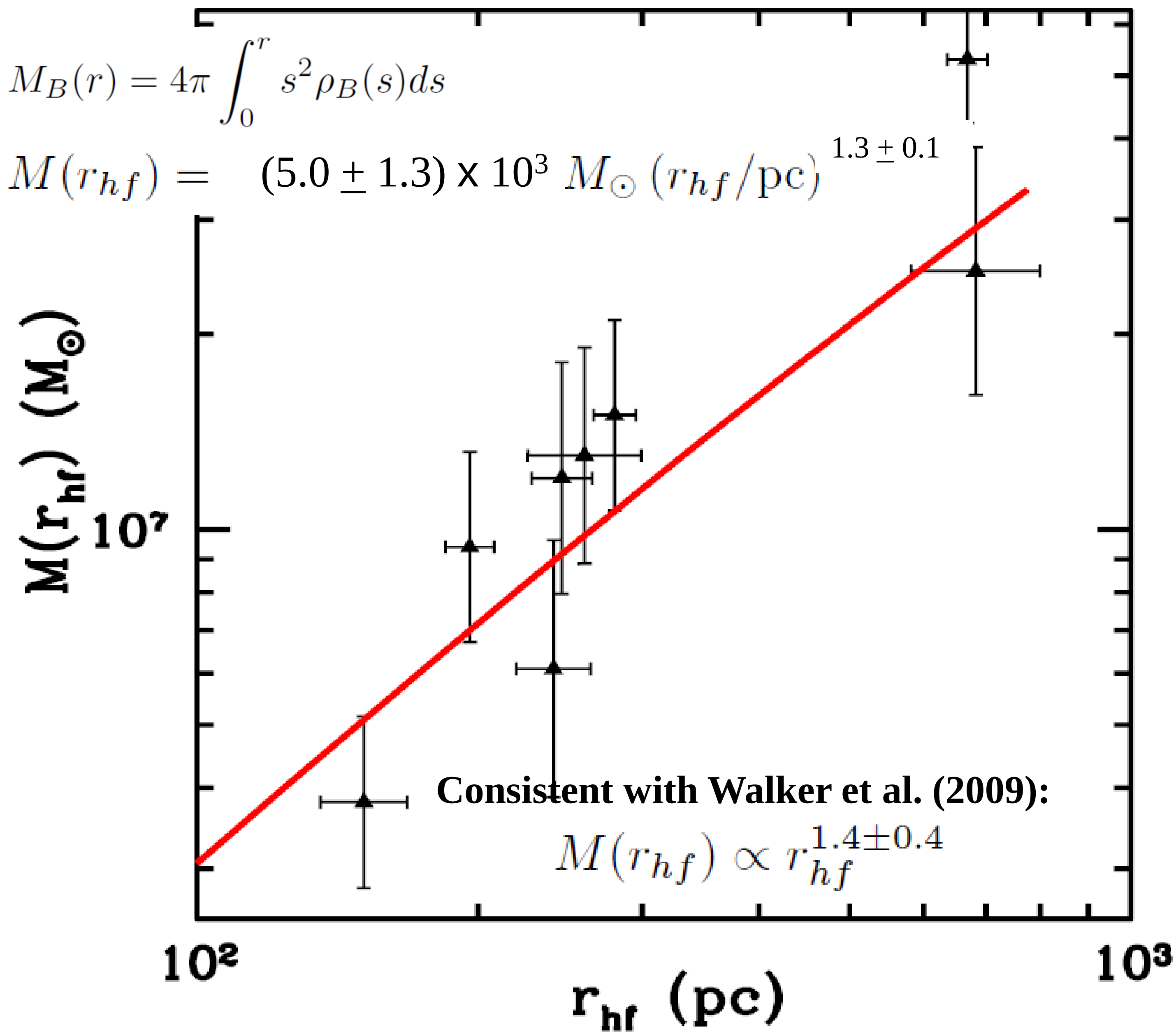

Consistent with Walker et al. (2009):

$$M(r_{hf}) \propto r_{hf}^{1.4 \pm 0.4}$$

Conclusions

DW excluded via M31 X-ray constraints and phase space density constraints from MW dSphs.

(Watson et al. 2012, Horiuchi, et al. 2014, This Work)

DM explanation of 3.57 keV line excluded.

(Urban et al. 2015, Carlson, et al. 2015)

Phase Space Densities of MW dSphs imply narrow range of keV-scale values for m_{DM} that can

- **satisfy all galaxy constraints**
- **evade Lyα limits**

Best-fit Burkert Profiles of MW dSphs indicate

- **strong correlations between observables and DM halo properties: $r_0(r_{hf})$ and $\rho_0(r_{hf})$.**

Extra Slides for Questions

Sterile Neutrino Interactions with SM Particles

(Abazajian, Fuller, Patel 2001 [5]; Abazajian, Fuller, Tucker 2001 [6])

Very small mixing ($\sin^2 2\theta \lesssim 10^{-7}$) between

mass $|\nu_{1,2}>$ &

flavor $|\nu_{\alpha,s}>$ states:

$$|\nu_\alpha\rangle = \cos\theta|\nu_1\rangle + \sin\theta|\nu_2\rangle$$
$$|\nu_s\rangle = -\sin\theta|\nu_1\rangle + \cos\theta|\nu_2\rangle$$

For $m_s < m_e$,

3ν Decay Mode Dominates:

$$\Gamma_{3\nu} \simeq 1.74 \times 10^{-30} s^{-1} \left(\frac{\sin^2 2\theta}{10^{-10}}\right)\left(\frac{m_s}{\text{keV}}\right)^5$$

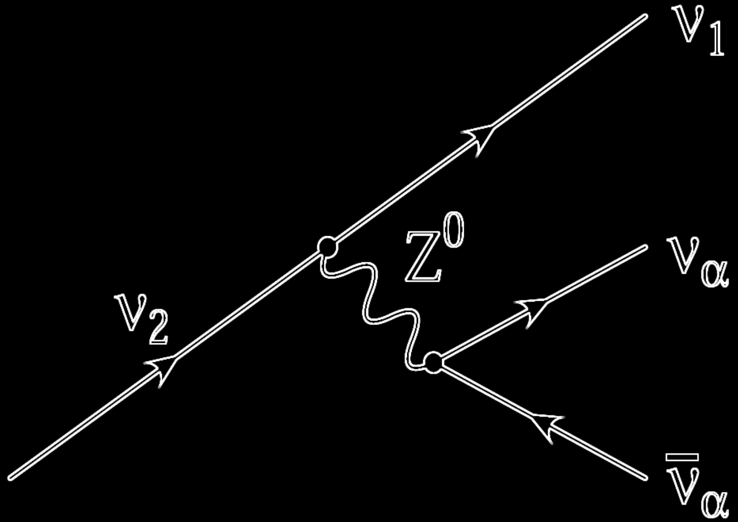

Radiative Decay Rate is:

$$\Gamma_s \simeq 1.36 \times 10^{-32} s^{-1} \left(\frac{\sin^2 2\theta}{10^{-10}}\right)\left(\frac{m_s}{\text{keV}}\right)^5 \quad \nu_s \rightarrow \nu_\alpha + \gamma$$

Andromeda's

Well-measured Matter Distribution:

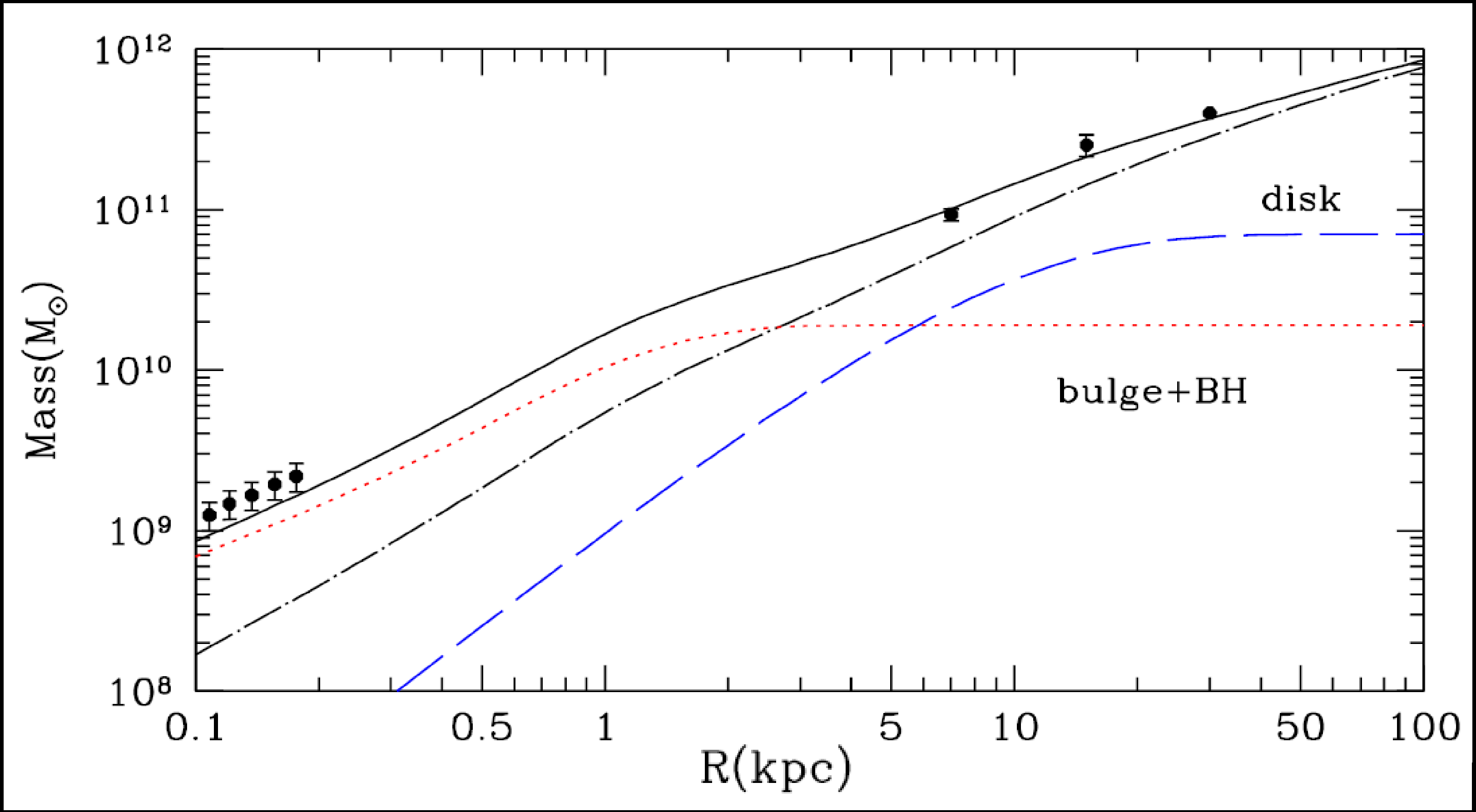

Constraints at small radii are from Stellar Motions in the Nucleus.
Three points at R>5 kpc characterize the spread in v_{rot} = 255 $\pm$ 15 km/s.

(Klypin, Zhao, Somerville 2002 [104] (KZS))

(Additional Data & updated analysis in Seigar, Barth, & Bullock 2007 [105] (SBB))

More Conservative DM Matter Distribution:

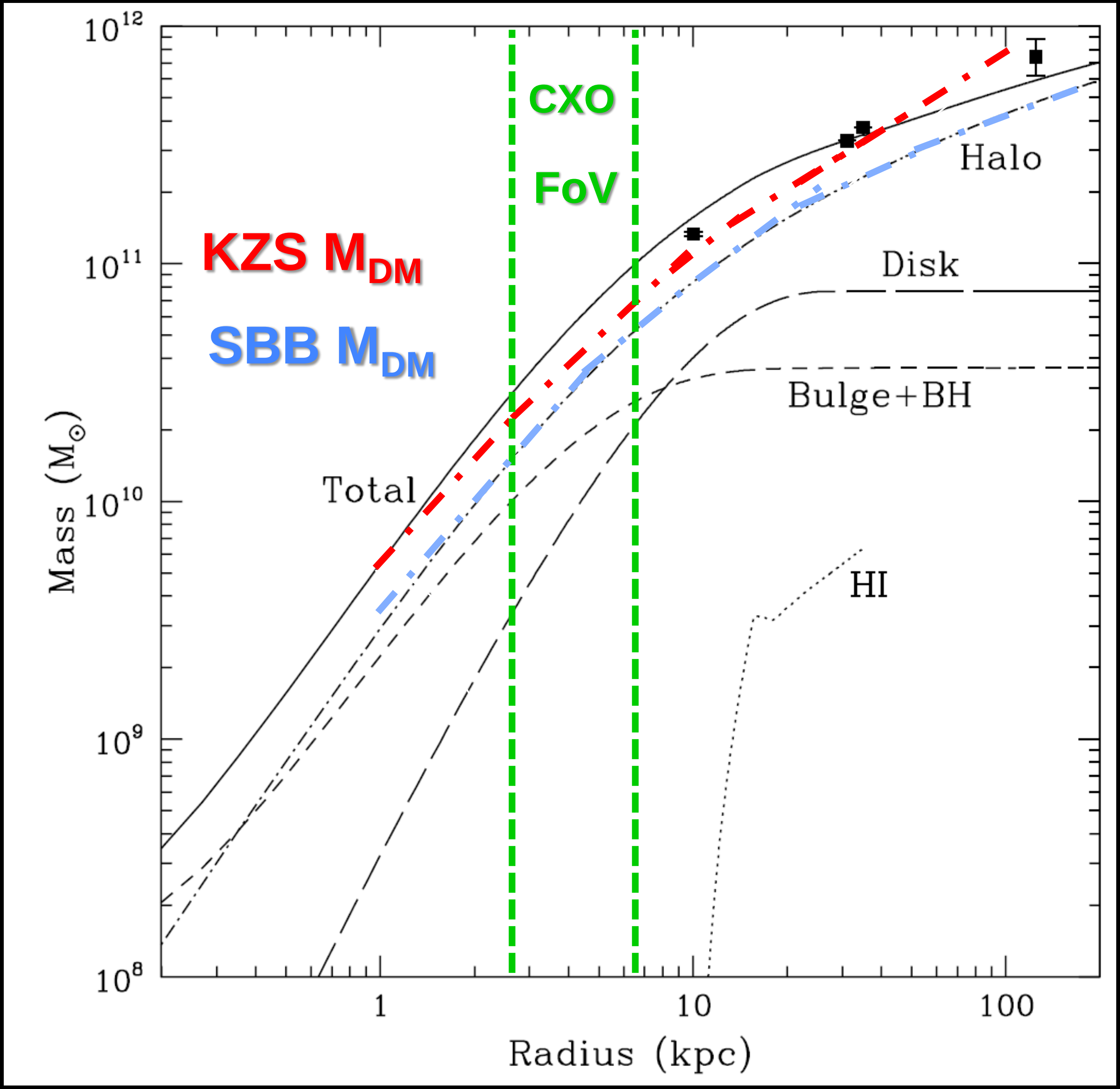

SBB M_{DM} [105]

<

KZS M_{DM} [104]

by a factor of

~ 1.05 – 1.2

in *Chandra* FoV

SBB M_{DM}

<

Burkert M_{DM} [67, 106]

by a factor of

~ 1.2 – 1.4

in *Chandra* FoV

Limits on m_s from *Chandra* Observations of M31

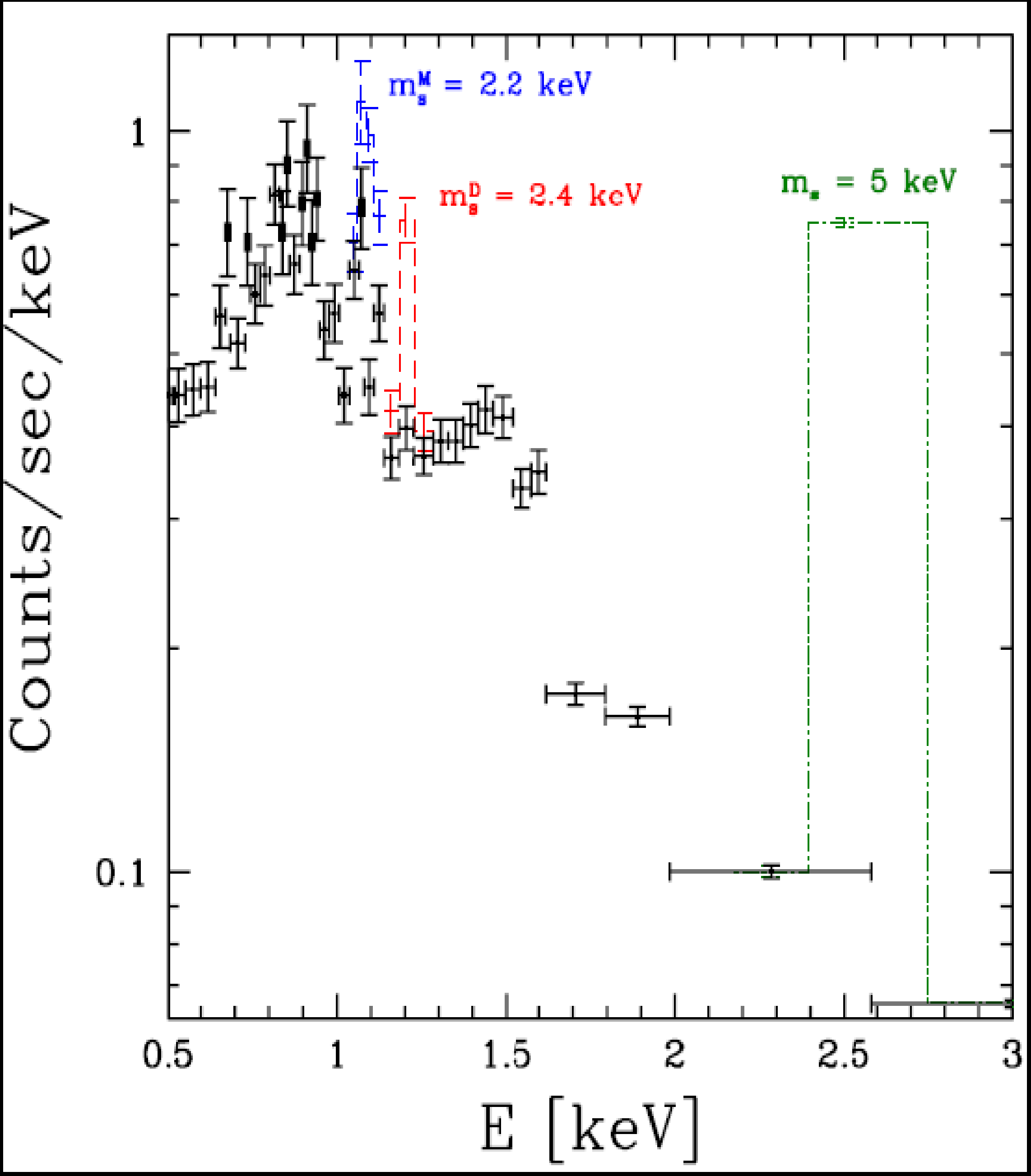

Chandra **unresolved X-ray spectrum emitted from 12' - 28' annular region of Andromeda (M31).**

Majorana:

m_s < 2.2 keV

Dirac:

m_s < 2.4 keV

Claimed Detection:

m_s = 5 keV

(Loewenstein & Kusenko 2010 [82])
STRONGLY excluded by our data!

Conversion of Decay Signal to Detector Units:

$$\frac{dN_{\gamma,s}}{dE_{\gamma,s}dt}(\Omega_s) = \left(\frac{\Phi_{x,s}(\Omega_s)}{E_{\gamma,s}}\right)\left(\frac{A_{\rm eff}(E_{\gamma,s})}{\Delta E}\right)$$

$$= 6.7\times 10^{-2}\ \text{Counts/sec/keV}\left(\frac{\mathrm{A_{eff}(E_{\gamma,s})}}{100\ \mathrm{cm}^2}\right)$$

$$\times\left(\frac{\Sigma_{\rm DM}^{\rm FOV}}{10^{11}M_\odot \mathrm{Mpc}^{-2}}\right)\left(\frac{\Omega_s}{0.24}\right)^{0.813}\left(\frac{m_s}{\rm keV}\right)^{1.374}$$

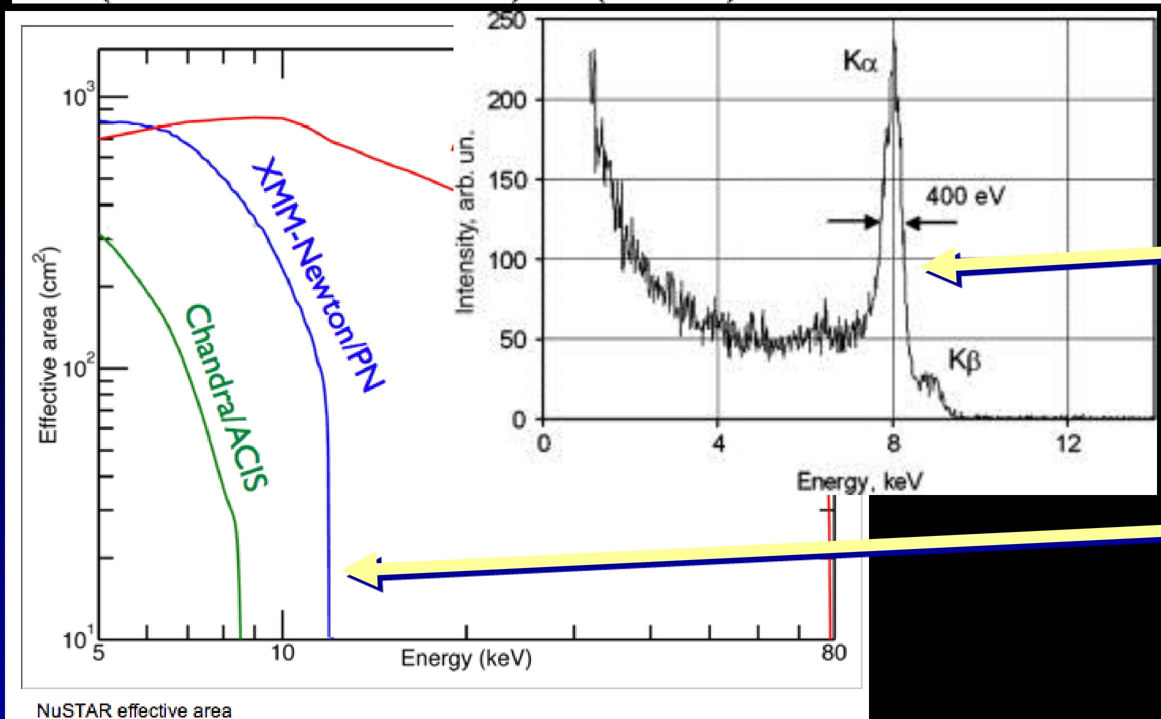

Detection of ν_s Decays at $E_{\gamma,s}$ depends on

- $\Phi_{x,s}$
- Spectral Energy Resolution $\Delta E \simeq E/15$
- ACIS-I Effective Area $A_{eff}(E_{\gamma,s})$

Detection/Exclusion Criterion:

$$\frac{dN_{\gamma,\mathrm{s}}}{dE_{\gamma,\mathrm{s}}dt}(\Omega_\mathrm{s}) \geq \Delta\mathcal{F}$$

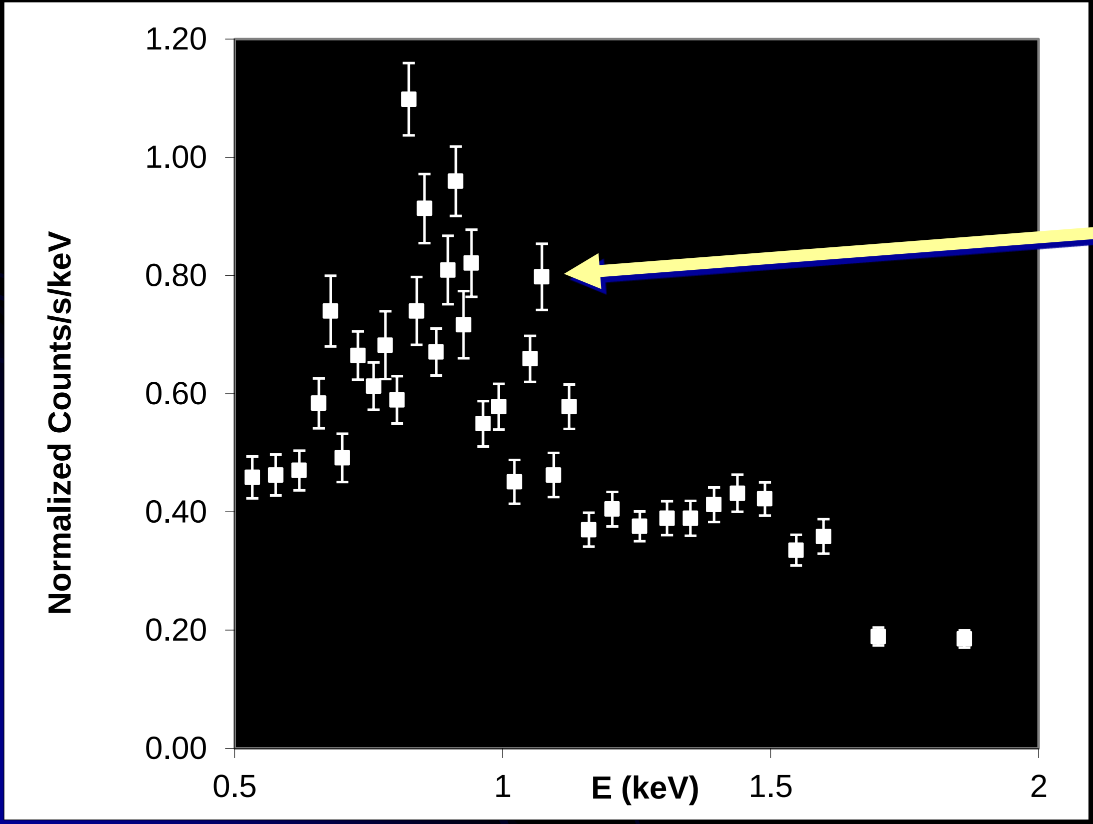

- Sterile Neutrino Decay Signal $dN_{\gamma,s}/dE_{\gamma,s}dt$
- $\geq$ *Chandra* Data $\Delta\mathcal{F}$
- in a given bin of energy $E_{\gamma,s}$